6 K program Final Report
NAS-5 99239

by

Dr. Willy Gully
Ball Aerospace

June 2001

Index

Executive Summary

There is a need for reliable, space qualified mechanical coolers for temperatures of 10 Kelvin and below for use in both x-ray and infrared systems. An example of the x-ray system is the sub-Kelvin Adiabatic Demagnetization Refrigerator, which provides a cold environment enabling calorimetric methods for detecting X-rays. This ADR cooler in turn requires a reject temperature of about 6K, and it is the goal of this program to design a cooler to meet this need.

Our analysis shows that the most efficient cooler for applications in a low Earth orbit is a hybrid cooler consisting of a helium Joule Thomson cooler coupled with a Stirling cycle mechanical cooler. We use the relatively mature Stirling cycle mechanical cooler to provide all of the pre-cooling, and employ the JT recuperative system for refrigeration to 6K, a region that has historically been difficult for regenerative coolers. This Explorer program focused on the technology development required for a suitable Stirling precooler. A parallel Air Force Research Laboratory program contributed to the development of the associated JT system.

Our Explorer Program ran from late 1998 to mid 2001. The program was a productive interplay of testing, analysis, revision, and re-testing. We developed techniques to handle and confine the lead and rare earth powder regenerators. We were able to characterize lead, rare earth (RE), and rare earth alloy (REAY)regenerators and compare our results with analytic predictions based upon the NIST developed Regen3.1 simulation program. And we were able to demonstrate cooling in the temperature range required for our precooler. The program therefore met all of its proposed goals.

Based upon these results, we were able to pick a Stirling operating point that is easily within our design space. With that anchor, we were able to flesh out the rest of the details of a 100 mW, 6 K cryocooler. We predict that a hybrid cooler designed to support a reasonably sized load will consume 200 Watts of input power and have a mass of 23 Kg. In this budget generous allowances have been made for parasitic loads resulting from supporting and shielding the load.

The first part of this final report is a compilation and discussion of our regenerator researches. The second part is a summary of our proposed hybrid cooler. In all, substantial progress has been made towards developing a long life mechanical cooler for use in lower temperature space systems.

ii. List of figures

I. Stirling Precooler Research

I. Stirling Precooler Research Program

A. Introduction

In this section we discuss our hybrid cooler approach, including the pivotal design constraints brought about by the long life requirements for a space system. We discuss the current conceptual design of the JT cooler, and how that influences the Stirling cooler architecture. We then provide some background material as a starting point for our work.

Motivation for a hybrid cooler: Our use of a hybrid system reflects the difficulties in achieving very low temperatures with a regenerative mechanical cryocooler alone. In a hybrid, the last stage of cooling is delegated to the JT. The Stirling cooler provides the JT's pre-cooling as well as the auxiliary cooling of the parasitic loads from the surrounding radiation baffles and support structure.

Our analysis suggests that the hybrid system can be designed to run with approximately the same power efficiency with the precooler operating anywhere from 12K to 16K. Our task is to learn what we can actually achieve with our precooler, and then design the JT system to handle the rest. Our goal is to design a hybrid cooler providing 100 mW of cooling at 6 K.

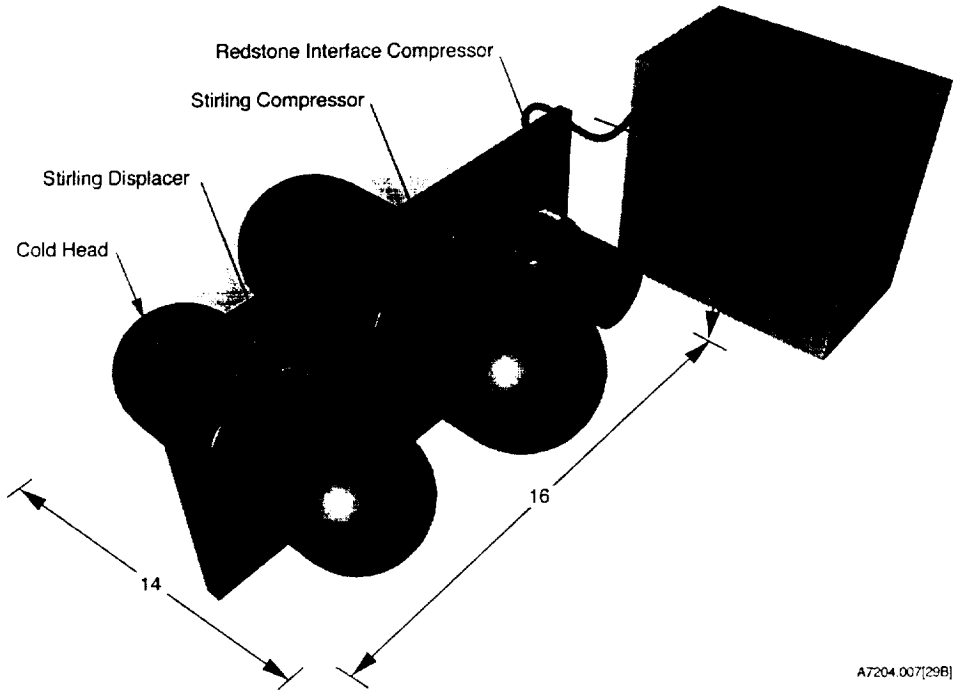

Figure 1. A conceptual drawing of a 100 mW 6K cryocooler showing the Stirling and JT coolers as well as the control electronics.

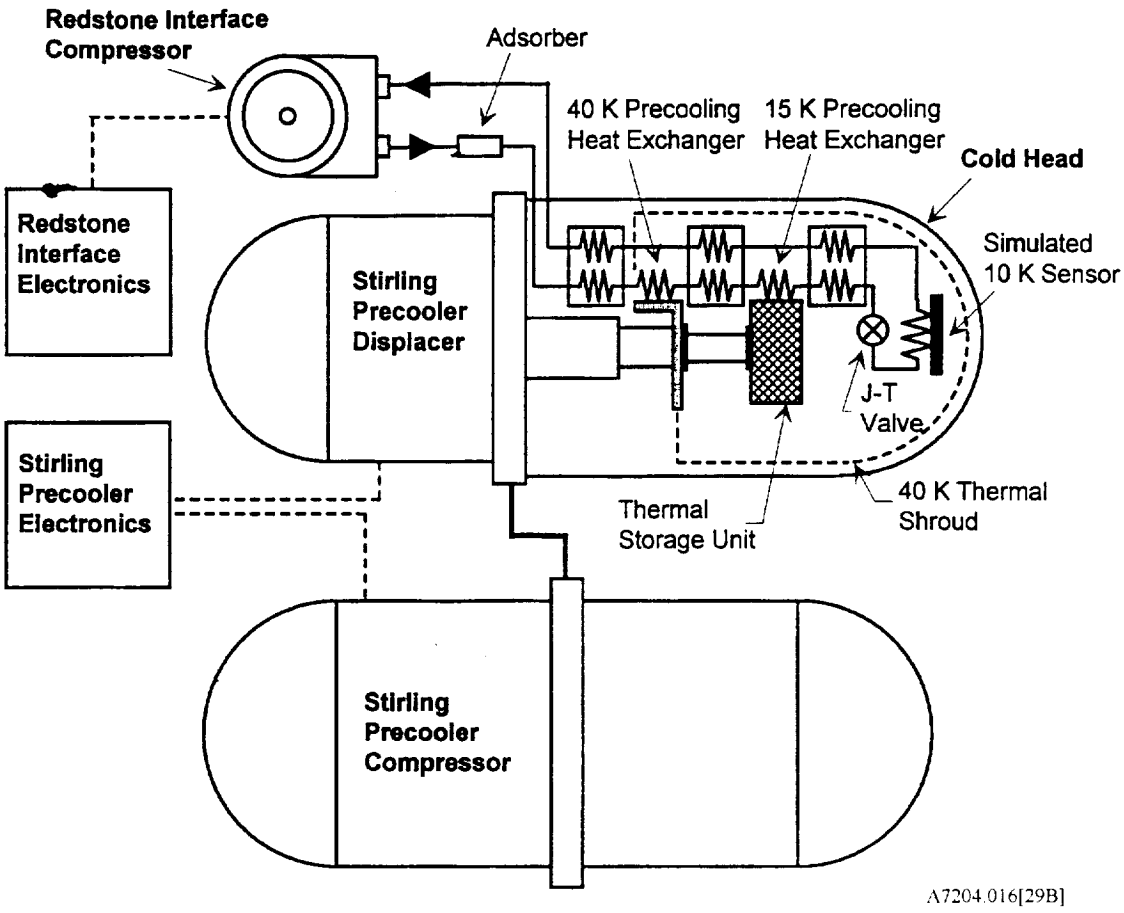

Figure 2. A schematic of a hybrid cryocooler. The Stirling cooler intercepts the losses due to the inefficiencies of the JT's heat exchangers, allowing it in turn to cool to lower temperatures.

Limitations of regenerative coolers at low temperatures: At these temperatures, the helium gas density increases substantially. For example at 10K, the density of an ideal gas would be 30x that of the gas inside the compressor at room temperature. And real gas effects, that occur because we are approaching the critical point of helium, increase it yet again by half. This has a number of consequences. Small nooks and crannies in the cold regions of the cooler become a problem because of the amount of mass required to fill them during the cycle. And as the matrix capacity falls away due to quantum effects, its is incapable of storing the internal energy of the working fluid, thereby destroying the efficiency of the Stirling cycle. In spite of these difficulties, regenerative coolers had approached 10K in the 1950's, and several commercial mechanical refrigerators can operate below 6K today.

What sets our cooler apart from previous work? What sets this investigation apart is that we are trying to achieve these temperatures with a long life, non-contacting, relatively high speed Stirling cryocooler. There are additional constraints associated with the use of these coolers since they are designed to operate without wearing seals in the compressor and in the cold head. Wearing seals are not compatible with reliable

operation for a long time. Wear leads to leakage, particulate debris, and even unwanted volatile gaseous contamination, all of which degrade the performance of the cooler. In contrast the non-contacting coolers have no similar degradation mechanism. However, they rely on a relatively high cycle speed to limit the mass flow through the small clearance gaps between pistons and cylinders. Our regenerator design has to be compatible with these gap clearances.

Non-contacting coolers are linear coolers. The mechanisms must oscillate linearly in order to avoid the "crank" that leads directly to large side loads that would compromise the gaps. Without side loads you can use diaphragm springs to support the armatures within their cylinders. However, to achieve this potential, the system must be fabricated and aligned carefully. Because of technology we developed on the NASA GSFC 30 K program, we have been able to demonstrate efficiently operating, non-contacting Stirling cryocoolers down to 30K with gaps <= 25 micron. However, in our current design we operate > 30 hz to support the pressure wave. This high frequency and relatively wide gap become serious design constraints for a cold head.

In contrast, commercial mechanical coolers easily provide watts of cooling at these temperatures. They can perform this well because a wearing seal at the cold tip enables them to operate at frequencies on the order of 1 hz. This is a distinct thermal advantage because there is plenty of dwell time for the heat of the incoming gas to diffuse into a compact matrix. There are several coolers that meet the proposed 6K cooler thermal requirements handily, but they are not adaptable to flight because their thermal design hinges upon the performance of this wearing seal.

The status of JT system work: As shown in Figures 1 and 2, the JT system consists of a room temperature circulating pump, high efficiency heat exchangers, and a JT expansion valve. All of these have been under development in parallel programs, and in this section we will briefly provide a status of that work.

At Ball we had a parallel "10K Cryocooler" program funded by the Air Force Research Laboratory, Kirtland AFB, New Mexico. Our goal was to develop the an analogous helium gas JT cooler and demonstrate its operation at 10 Kelvin. Since we yet had to do the precooler technology development work, we expected to use a commercial GM cooler to support the JT system we were developing. The JT cooler we propose for the 6K hybrid cooler is based upon the compressor developed on this 10K program.

Status of the helium circulating pump: Prior to our work on 10K, there simply was no circulating pump suitable for "dry" cryogenic operation. Departing from the non-contacting philosophy of our Stirling coolers, we chose to develop a "contacting" but still "long life" helium gas circulating pump based on rotary vane technology. The key idea is to employ the demonstrated low wear obtained with properly lubricated graphite vanes.

We built and characterized a prototype circulating compressor on the 10K program. The pump is shown in Figure 3. The pump worked reasonably well, given the radical departure from the current state of the art. Most goals were met, but some work remains

on an internal bearing. At present the pump delivers half the flow required for a 100 mW system, but would readily meet the requirements if brought to its design potential.

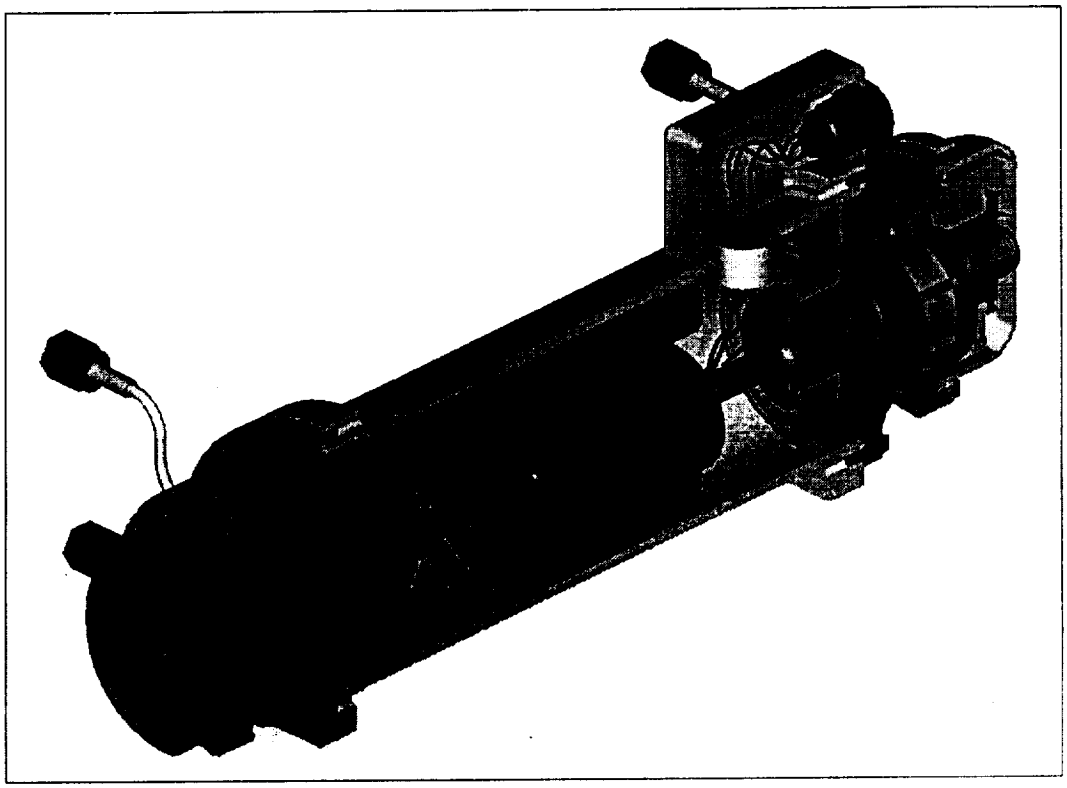

Figure 3. The two stage Helium gas circulation pump developed on the 10K AFRL program.

Status of the cold head design: The cold head consists of the room temperature plumbing, the heat exchangers, and the JT expansion valve that make up the rest of the JT cooler system. They were originally part of the 10K program, but were later dropped as we concentrated on the compressor. In this section we discuss the status of these parts.

a. ***Gas Handling system:*** The room temperature gas handling system consists of lines, storage tanks, and in-line elements that filter and purify the gas. A gas handling system was designed but not built on the 10K program, but enough information exists for a rapid design for the 6 K cryocooler.

b. ***Heat Exchangers:*** Heat exchangers are used to isolate the cryogenic system from room temperature. The cold gas exiting the cold head pre-cools the warm gas coming in to replace it. Heat exchangers were designed and built on the 10K program. But we also uncovered a promising new approach that is now being pursued by Redstone Engineering on a small business contract. These new exchangers, developed at NIST, are uniquely

compatible with the 6 K system. We assume that these exchangers will be available and use them in our baseline design.

The heat exchangers influence the precooler design in two ways. The precooler has to intercept the heat due the heat exchanger inefficiencies. For example, we could use a more powerful Stirling cooler to absorb the loads from less efficient heat exchangers if their cost and complexity were the primary concern. The precooler also has to intercept the radiative heat load that falls on the shields that surround the cold head. This envelope is driven by the heat exchanger size. The NIST exchangers are quite attractive because of their relative compact size.

We have planned for system efficiencies resulting in a cooler with 2000 watts/watt of cooling at 6K. This requires three heat exchangers with efficiencies >= 99%. The resulting heat loads are dumped onto the Stirling stages at 180K, 40K, and 14K. These exchangers will be discussed in Part II of this report.

c. *Cold head:* We have based our design on a JT expansion valve designed and tested at Ball a decade ago. A separate heat exchanger connects the cold effluent of the valve to the system to be pre-cooled. Since a satisfactory flight design exists, no current effort is underway on its further development.

Starting point for these investigations:

In the preceding section we outlined some of the constraints on the precooler: high speed and clearance gaps, three stages to intercept the heat from the JT heat exchangers, and a cold tip operating between 12 to 16K. We were in a strong position to undertake the development of this precooler because we were in possession of uniquely applicable hardware.

In a follow-on subcontract to our original "30K" Stirling development program, we were asked to develop a multistage cooler capable of simultaneous refrigeration at both 35K and 60K. If a cooler can carry multiple loads, it cuts down on the number of coolers in a system. To meet the efficiency requirements, however, we had to develop a cooler with a third expansion stage. [W.J.Gully, H. Carrington, and K. Byrne, "A mechanical cryocooler for dual temperature applications", STAIF pp 205, 1998, AIP conf. Proc. 420.]

The three stage breadboard displacer/regenerator assembly we created on the 35/60K program was the perfect test bed for the 6 K precooler. The first two stages operated in about the right range already, and by suitable regenerator changes we felt we could drop the last stage from 35 K to the 12-16 K range required. The 35/60K breadboard displacer regenerator assembly is shown in Figure 4.

Note that there is a bolted flange at nearly every interface, which allows for rapid prototyping of regenerators and interface details. This has been quite convenient for characterizing materials and configurations. However, the flexibility has a down side. The open nature of the breadboard, and the numerous o-rings required to seal the many de-mountable joints led to intermittent bouts with gaseous contamination. In each instance we were able to tell when we had contamination problems, and were always able to resolve the problem.

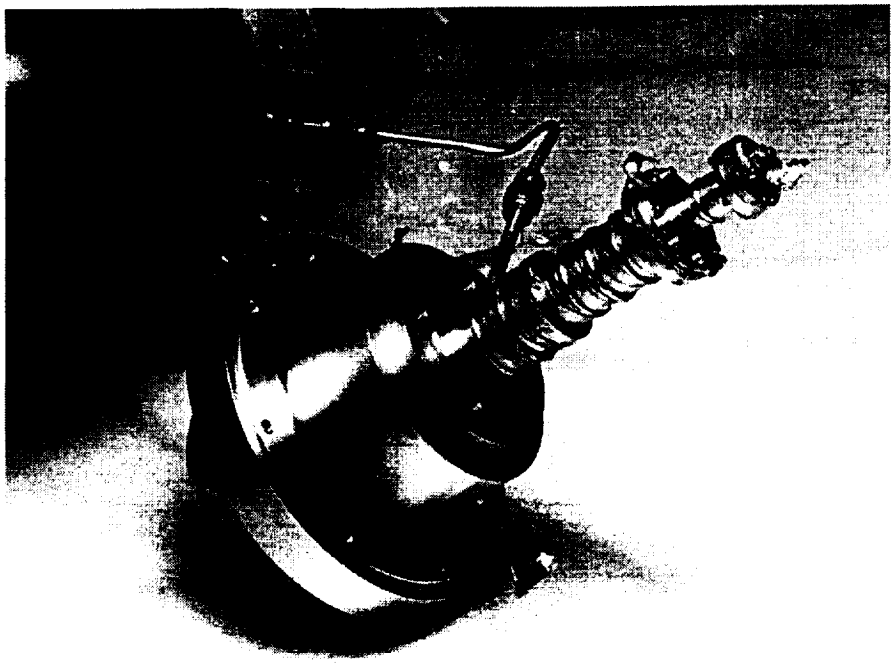

Figure 4. The Ball breadboard displacer used as a test bed during the 6K contract.

In Figure 4 we show the breadboard that we used to develop the 35/60 K cooler thermodynamic performance. Once we had arrived at a successful configuration we built the proto-flight version of this cooler, which is shown in the next figure 5. This cooler went through a thorough qualification test program, and is currently on life test at Phillips Laboratory, Kirtland Air Force Base, Albuquerque, NM. The proto-flight cooler demonstrates all of the attributes required for a true qualified space cooler, and shows that there are no roadblocks in developing an appropriate Stirling cooler for the 6 K program.

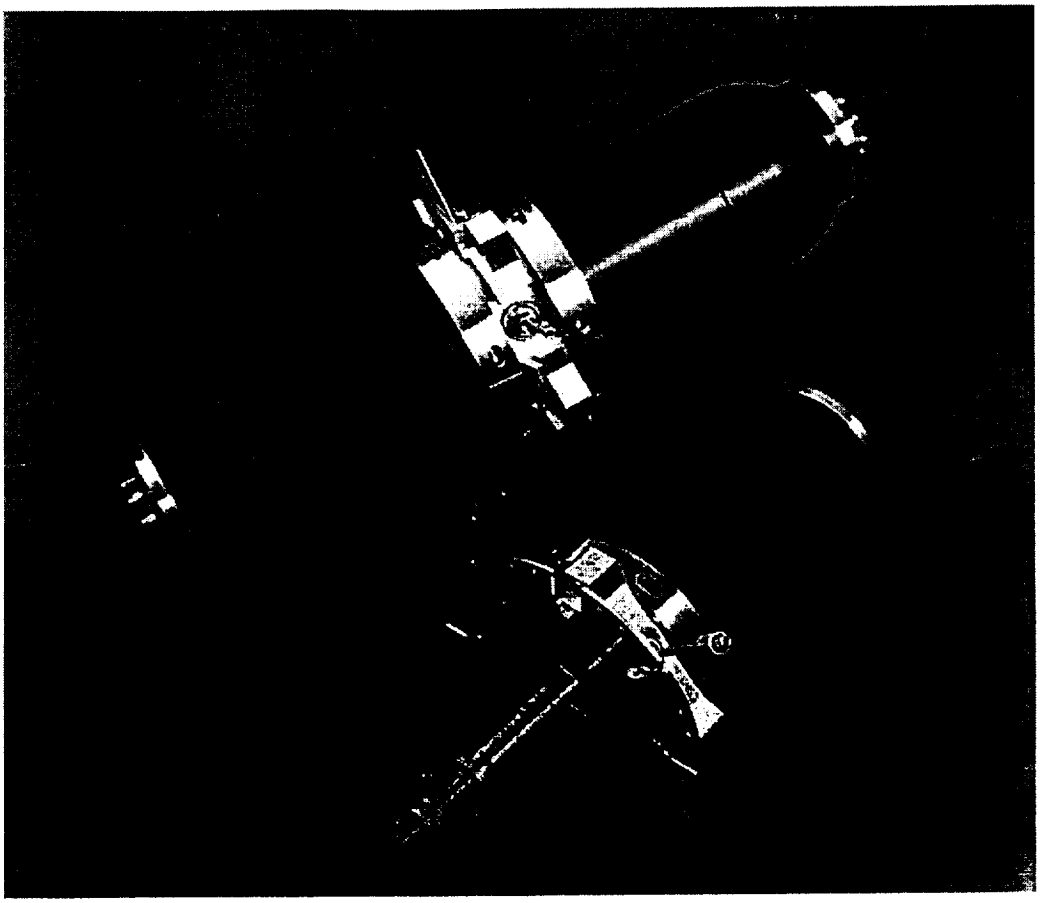

Figure 5. The proto-flight 35/60 K cryocooler based on the breadboard cooler shown in Figure 4 demonstrates that the Stirling Technology is mature.

B. Approach

In this section we provide some background to motivate our experiments. We begin with a tutorial on the salient factors that limit a Stirling refrigerator's performance at low temperatures. We then move on to the analytical tools used to model these coolers. In essence, the precooler work was done to provide first hand knowledge about various terms in our models. Finally, we provide model predictions made before this 6K program. These will serve as benchmark with which to compare our subsequent predictions.

Basic cycle: The essential elements of a Stirling cooler, the compressor and displacer, are shown below. A compressor moves the pressure up and down. In between pressure changes the displacer shuttles between the warm and cold ends of its tube, moving the gas to where it isn't. The displacer is depicted as lined, representing an internal regenerator with passages that allow the gas to flow through it.

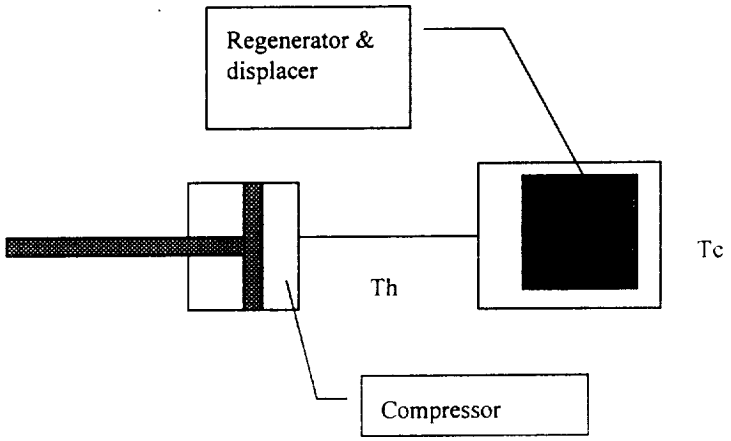

Figure 6. A compressor, displacer, and regenerator make up a Stirling cycle refrigerator.

If it weren't for the motion of the displacer the pressure oscillations would produce no cooling. The displacer shifts in such a way that the expansions always occurs when the gas is in the cold end of the displacer housing, and the compressions occur when the gas is in the warm end. This separates the compression and expansion events and leads to refrigeration at the cold end of the displacer. The gross cooling power is given by the frequency times the work $\int pdV$ that occurs in the cold end.

The regenerator is a key element of the Stirling cooler. Its function is heat recovery. It ideally absorbs heat from gas moving from the warm to the cold end of the displacer. It returns this heat after the expansion when the gas is shuttled back to the warm end. This allows the expansions to take place at a much lower temperature than would be otherwise possible, and leads to an efficient machine.

There are limitations to how far a Stirling cooler can cool. As the temperature difference Th-Tc becomes large, heat flows down the cold finger and eventually offsets any cooling produced by the expansion. There are three principal losses. There is ordinary conduction. There is a "shuttle" heat leak caused by the intrusion of the warm displacer into the cold space. And there is the regenerator loss, caused by the inability of the regenerator to thermalize the incoming gas. The regenerator loss is critically important at low temperatures, and is a primary concern in this work..

There are many advantages to using a multi-stage cooler for low temperature work. It has a fundamental thermal advantage because parasitic heat is intercepted at expansion stages that occur at intermediate temperature, resulting in a more efficient system. It also naturally divides the cooler into segments, making it easier to tailor a regenerator for each temperature region. Finally, it divides the total temperature drop among the stages, minimizing the temperature span across the last stage where the regenerator loss is so important.

A sketch of our multistage cooler on a vacuum test enclosure is shown in Figure 7. A twin piston linear compressor is connected to a three stage displacer through a small diameter transfer line. There is an expansion stage at each step in the displacer. There is a separate regenerator between each stage. Our regenerators are "stationary", ie. , not moving with the displacer piston, as shown in the figure. In reality these regenerators are annular in form and surround the displacer cylinder tube. We repeat that the cryocooler has to be designed to support the clearance gaps shown. Our approach is to build a regenerator that can operate in parallel with the gap without losing a disproportionate amount of mass flow to it. In this way the gap becomes an extension of the regenerator and drops out of the problem.

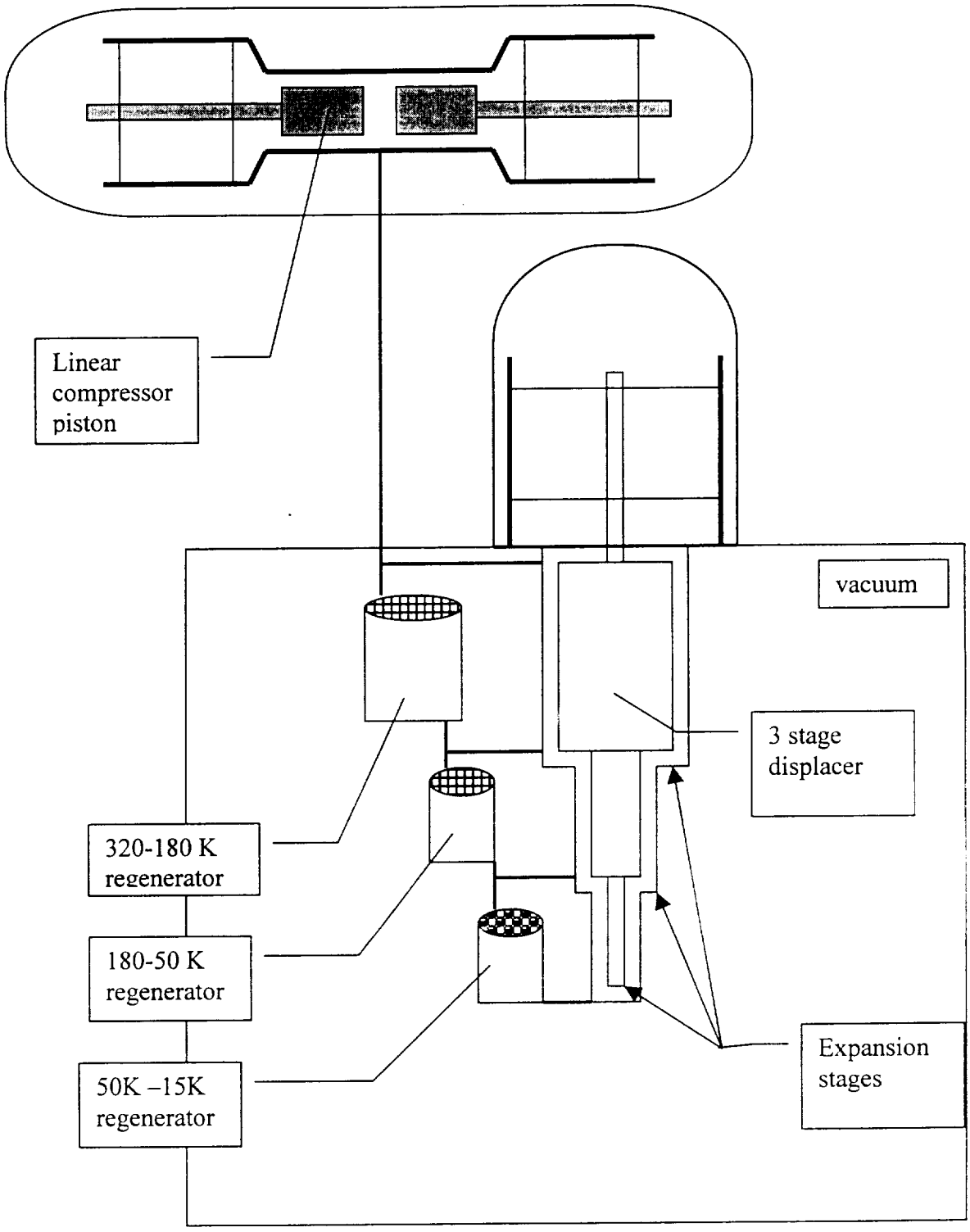

Figure 7. A representation of the 3 stage Stirling cycle cryocooler used during the 6 K program.

Fundamental design issues

The cooler works better if you can design it to use the minimum amount of mass flow possible. The cooler bottoms out in temperature when the losses increase to the point where they consume all of the gross cooling. Below 50K the dominant loss is due to the regenerator, and the regenerator loss increases quickly with mass flow. For a given configuration the shuttle and conduction losses are essentially a constant, so minimizing mass flow results in the most net cooling. We can write down a simple analytic expression for the net cooling, using an isothermal model of the expansion and an NTU model of the regenerator:

Gross cooling = = mdot *Tc* {S(Ph)- S (Pl)} = mdot * RTc * Ln Ph/Pl

Qregenerator loss = mdot Cp* (ΔT) * 2 *(pAf/A)* (1/Nst)*)*(1/(1-Cmin/Cr))
= regenerator geometry coefficient * mdot $^{4/3}$ * (1 / (1-Cmin/Cr))

Net cooling = mdot * RTc*Ln (Rp) – coeff * mdot $^{4/3}$ * (1 / (1-Cmin/Cr))

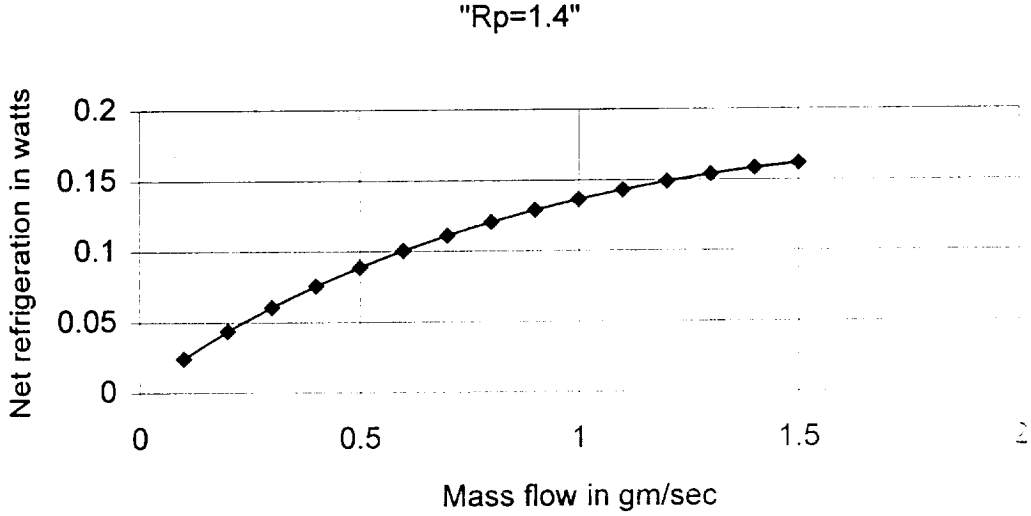

Figure 8. The net cooling saturates as a function of mass flow for a given cooler. Adding more power can actually make the cooler warm.

Consider the Stirling cycle as performed by the hardware in Figure 6. The mass flow into the cold end through the regenerator is crudely given by

dM cold = ((Ph-Pl)/RTc)*Vc + (Po/RTc) * dVc

The first term comes from pressurizing and de-pressurizing a static cold volume Vc, and the second comes from the flow due to the shift in the displacer's position. The cold work is given by (Ph-Pl)* Vc. Since (Ph-Pl) = 2*Po*(Rp-1)/(Rp+1), the same work can be obtained either by having a high pressure Po and low pressure ratio Rp, or by having a low pressure and a high pressure ratio. The latter case has less mass flow for the work,

which leads to a lower regenerator loss and more net cooling. One of the improvements we made was to increase its pressure ratio by using a larger compressor.

The above discussion is simplified. One has to do a complete analysis to understand all of the trades that lead to better performance. The simple model ignores pressure drops through the matrix, and that there are three different regenerators which cannot all be optimized at the same time. But it does depict many of the phenomena we see clearly in the last stage at low temperatures.

Another way to minimize the mass flow and improve the cooling is to reduce the porosity of the regenerator matrix. We did this when we converted from screens to powder, which dropped the porosity from 65% to 38%. We also used fine powder to get as much surface area A as possible, subject to the constraint that we had to limit the pressure drop across the last regenerator stage. In this way we minimized the thermal resistance between the gas and the regenerator matrix, making it more efficient.

Finally, we selected special materials to enhance the specific heat per unit volume of the matrix. The function of the regenerator is to store the heat from the fluid as it passes through to the expansion space. Since the porosity is fixed, the key is to have as much heat capacity in the remaining volume. If not, the matrix temperature goes up as the gas deposits its heat, which results in extra parasitic heat getting dumped into the cold expansion volume.

We must insure that the matrix capacity rate Cr = N* Cmatrix is large compared to the capacity rate in the flowing fluid, mdotCp. In Figure 9 we compare the specific heat of a cc of 10 Atmosphere helium gas with the specific heat of an equivalent volume of matrix. We see that steel and phosphor bronze are rapidly becoming unacceptable because of this effect.

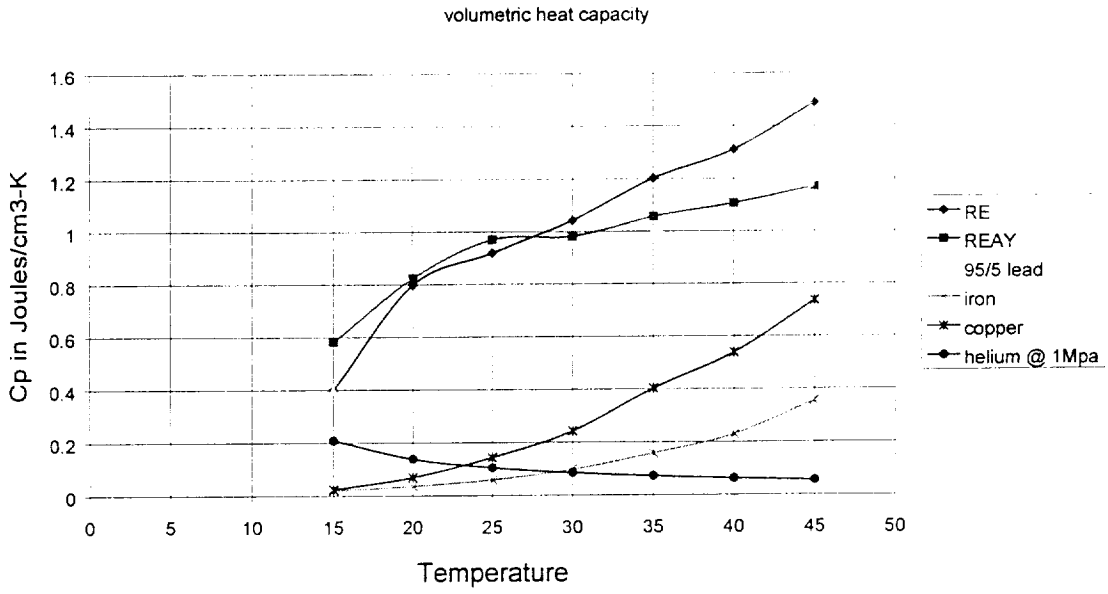

Figure 9. Heat capacities in the range of interest for materials commonly used in regenerators. Steel and brass regenerators are unacceptable below 20K.

Analytic tools used to model these coolers.

The cooler performance is given by

Qnet $= \int pdV\ N - \{ Qshuttle + Qconduction + Qregenerator \}$

Gross cooling, $= \int pdV\ N$

The gross cooling is the work performed at the expansion stage. We use a time difference thermo-mechanical models with a dozen nodes to track the pressure of the gas within our machine as time evolves. We run the model until it achieves a steady state and interrogate it for the pV diagram.

In order to allow for real gas effects in our model, we start with a differential form of the compressibility Z = (P/RT)/(M/V). We use it to relate mass flows to shifts in volume and pressure. We parameterize the modified equation of state with helium's virial coefficients. A plot of Z for helium in our operating range is shown below in Figure 10. As we begin to approach 10K, helium at 10 atmospheres begins to become non-ideal.

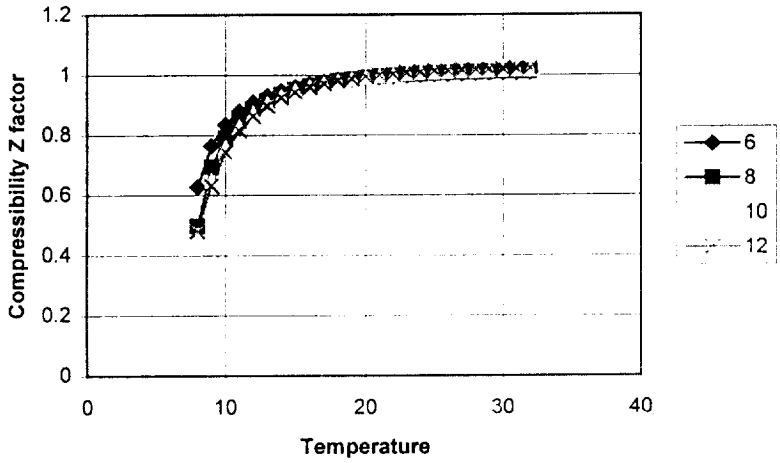

Figure 10. Compressibility Z = ρideal/ρ as a function of temperature and pressure.

As can be seen in Figure 10, at 10K the real density is greater than that you would calculate for an ideal gas filling that volume by about a third. This leads to an increase in the mass flow required to support a pressure change in that volume. This increase in mass flow is a problem because it further increases the regenerator loss above the amount calculated for an ideal gas.

Another real gas effects is the pressure dependence of the enthalpy, as shown for helium in Figure 11. We will re-visit the same expression in the context of our Joule Thompson cooler in the second section of this report. There are two consequences of this effect that tend to cancel each other out.

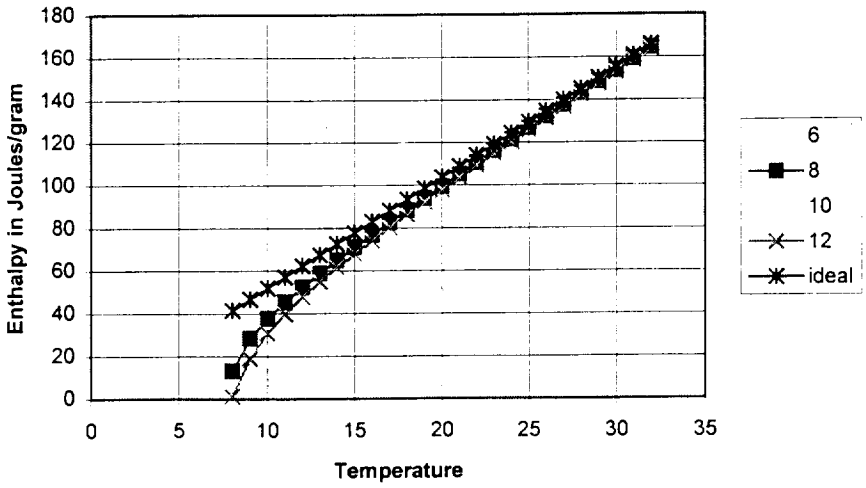

Figure 11. The enthalpy of 4He becomes a function of pressure near 10 K.

The first apparent effect is what appears to be bonus cooling due to a change in enthalpy with pressure. If cold gas enters the expansion space at high pressure and leaves at low pressure, Figure 11 shows that there is an enthalpy current out of the cold volume simply because the exiting gas has greater enthalpy. This bit of extra cooling is a vestige of Joule Thompson refrigeration.

We also have to consider what effect this has on the performance of the regenerator. In Figure 11 we see that Cp = dH/dT is higher for the high pressure stream than for the low pressure stream. Therefore, the cold "exhaust blow" is not able to remove the heat brought into the regenerator by the warm "incoming blow". This fundamental imbalance destroys the effectiveness of the section of regenerator in which it takes place. The regenerator is repetitively asked to store more heat than is removed. The consequence must be that the regenerator drifts in temperature until the heat leak to the cold expansion volume balances out. The resulting extra heat loss is "the flip side" of the extra expansion enthalpy and basically cancels it out.

In summary, we have developed a real gas thermo-mechanical model that we use to predict the pV diagrams that occur in the cold head. The work in these diagrams gives the gross cooling power. We discount the extra cooling power one naively calculates from the enthalpy current, assuming that it is offset by the extra regenerator loss due to the imbalance in the streams.

Shuttle Loss

We use an expression due to Zimmerman and Longsworth to account for this minor loss in our machine.(Adv.cry.eng16, 342-351) The loss is given by Qs = .186 * Khe * (2 *pi*R/δ) * Y^2 *(Th-Tc)/L where Y is the p-p stroke, R is the radius of the displacer, L is the length of a stage, and δ is the gap between the piston and the wall.

Conduction Loss

It would seem that it would be straight forward to calculate the thermal conduction along the materials that make up the cold finger. This is true for solid materials, but the largest section belongs to the regenerator beds, which consist of layers of materials. It is somewhat more difficult to calculate the losses for these regenerator beds. We begin with a collection of material conductivities in the range of interest.

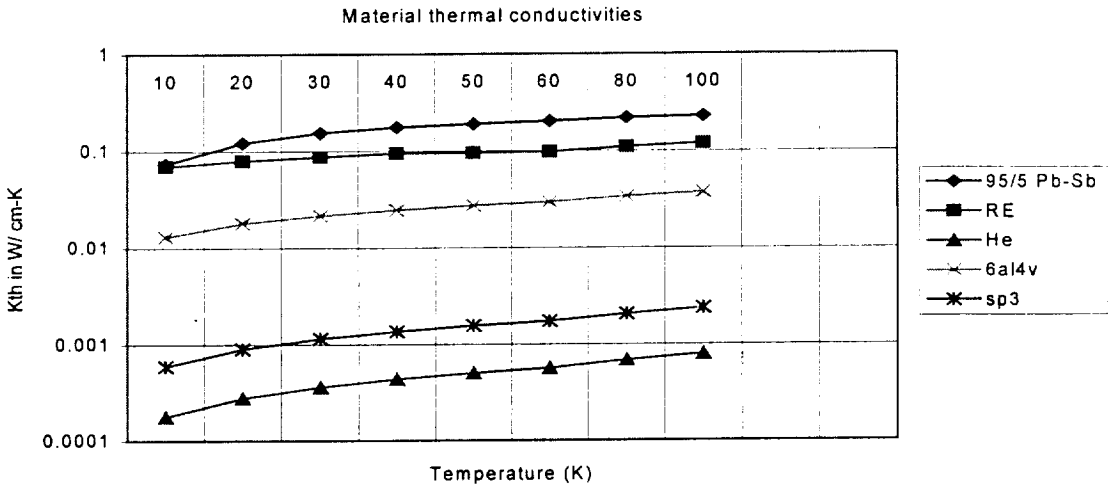

Figure 12. The thermal conductivities of bulk materials of interest.

Helium gas and Dupont Vespel SP-3 have low conductivities. 6Al4V Titanium alloy also has a low conductivity and is extensively used as a structural material in our cold fingers. The bulk conductivities of the regenerator materials are an order of magnitude higher.

The key fact to appreciate is that the conduction down a regenerator bed made from these materials is not nearly as bad as the bulk conductivity would indicate. McAdams (Adv.cry.eng. 13,p587) found that the bed conductivities were much reduced because the heat had to repetitively pass though the layer of gas between metal layers. In this sense the bulk conduction is better modeled as a shortened column of gas. Results for various beds are shown in Figure 13.

Regenerator Loss:

We have made extensive use of a program developed at NIST called Regen3.1. This is a 1-d simulation program that models the physics of the cyclic gas flow interacting with a matrix. We start with values of the regenerator mass flow that we get from our thermo-mechanical model. We run Regen3.1 until it achieves a steady state heat flux along its length. The regenerator loss is the enthalpy current due to the mass flow at the cold boundary. One of the achievements of this work is that we have been able to compare our results to the predictions of Regen3.1.

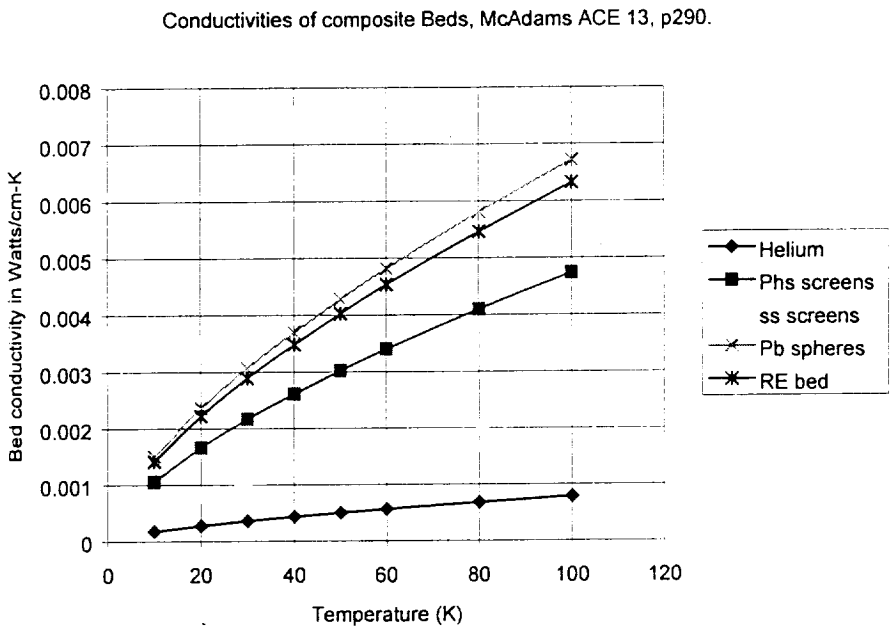

Figure 13. The effective conductivity of material beds is best expressed as a multiple of the helium gas filling them.

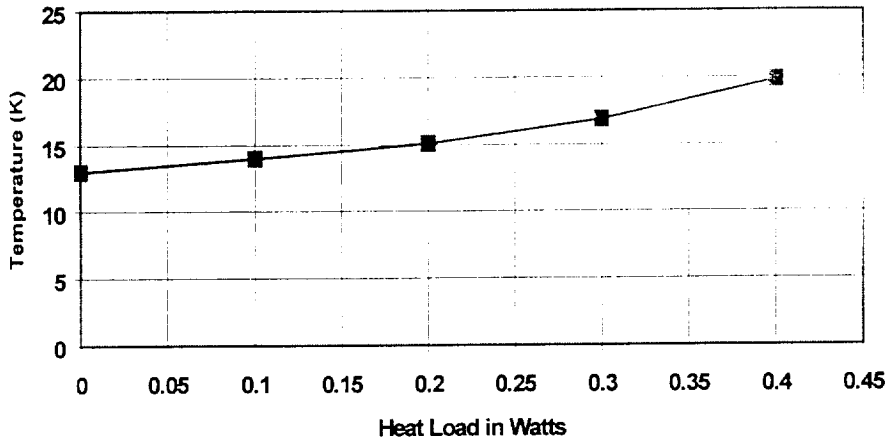

Figure 14. Early predictions for the "test 2" configuration.

We sum up this section with a prediction for the performance of our Stirling cooler pre-dating this program. It is to be compared with the results of our Test 2 configuration. It was optimistic in that it predicted a no load temperature of 13.5K and 200 mW of capacity at 15K. We have not been able to do quite as well, and it is of interest to understand why.

C. TEST PROGRAM

1. Road Map

The 6 K Program ran from October, 1999, to July, 2001. During that time we carried out six experiments that spanned the proposed activities. Each consisted of a fabrication effort followed by several runs to characterize the configuration and an analysis phase to digest the results. To summarize the program in a glance, I provide a table of key results below, a time line in Figure 15, and a sketch showing each hardware change in Figure 16.

Test	Date	Change	Expectation	Result	Comment
1	12/99	rebuild baseline 35/60	Characterize screen regenerators <= 20K	limited to 17 K	establish baseline, learn about dead volume
2	3-5/00	add lead shot regenerator in last stage	+ 400 mW cooling, and 4K lower temps	+ 75 mW cooling, and 2K lower temps	More needed than just lead in the regenerator.
3	7-8/00	Test 2 Configuration with larger compressor pistons	follow promising cooling trends with stroke	Best results	< 14K
4	10/00-2/01	Add RE to the midstage of the Test 3 configuration	assist cooling midstage which should help cold tip	Disastrous for both stages	Either flow blockage or contamination
5	2-3/01	Repeat original test 3 configuration; Then test RE, lead at cold stage	Reconfirm test 3 results; Then test larger particle size regenerators	Good test results	Repeat test 3, then find that larger particles don't work as well
6	4-5/01	Test 3 config with Reay cold regenerator	Should be better than lead	Comparable	Developed Qreg method

Table 1. A shorthand summary of the key results of each test.

Figure 15. Road map of the 6 K Explorer program experiments.

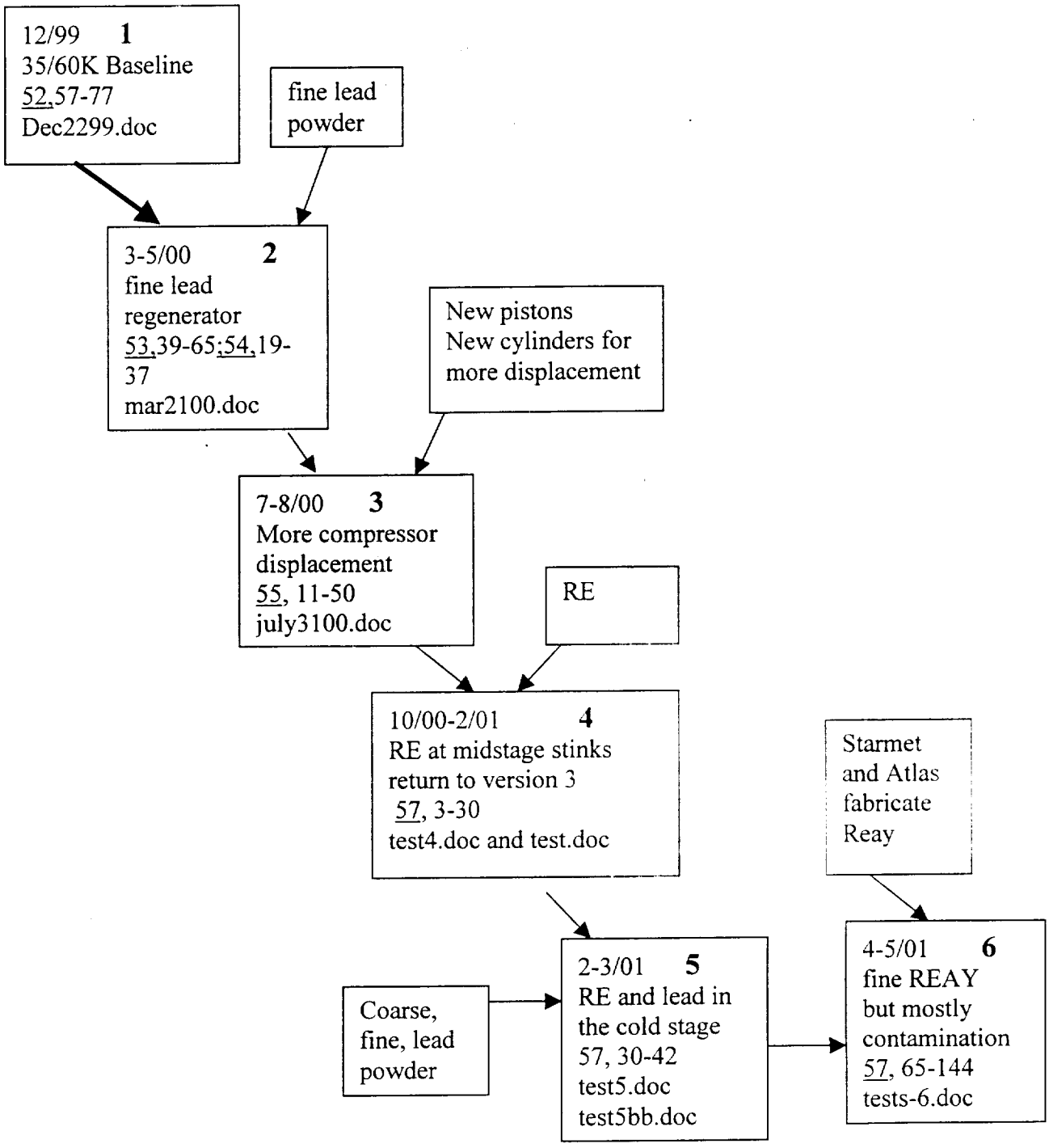

Figure 15. Each test involved a characterization of a physical change to the cooler.

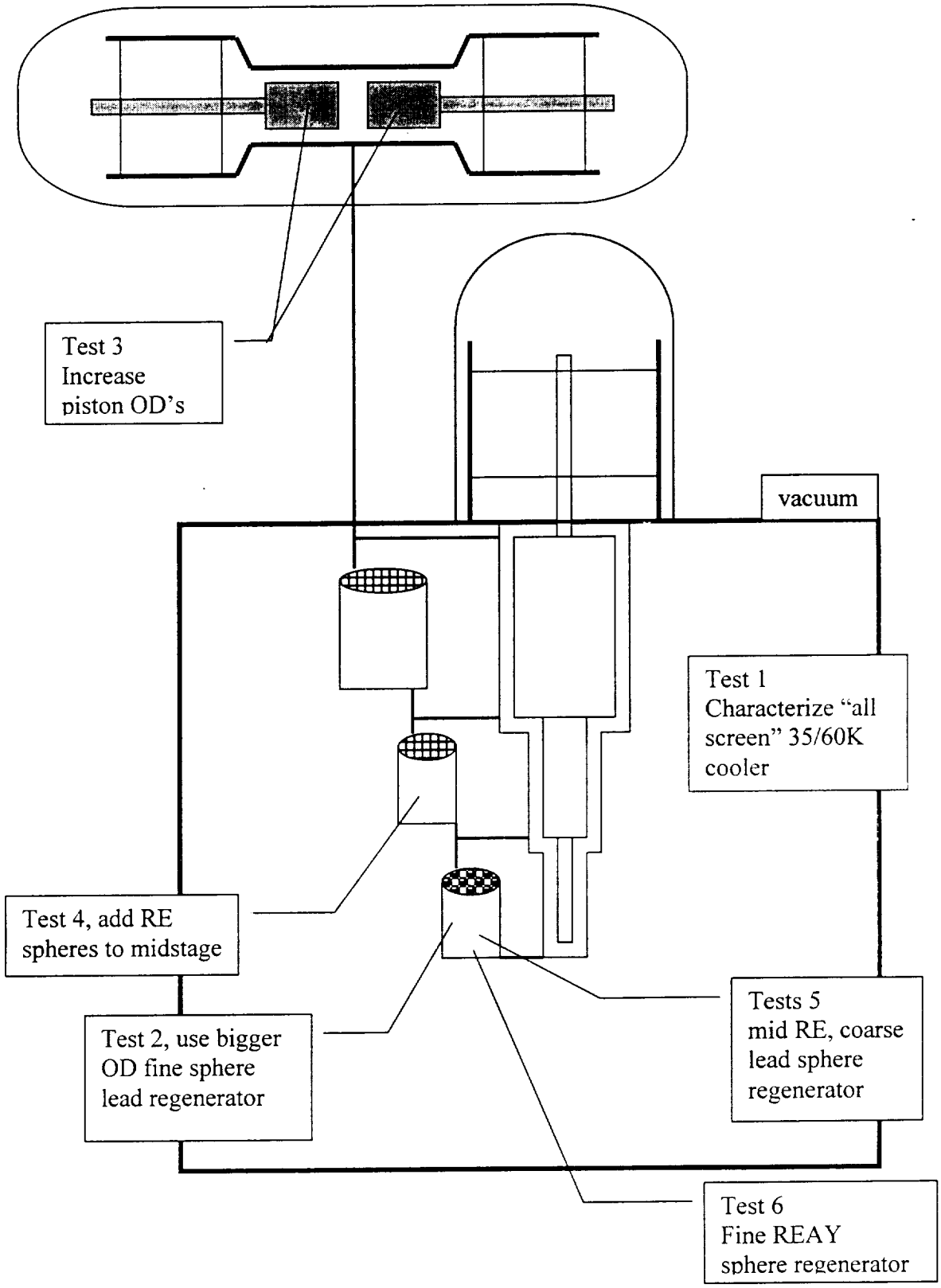

2. Test Plan

It is relatively difficult to inter-compare a long series of cryocooler experiments because a cryocooler is so complex that it is not likely that everything is under control. This is particularly true in a setup like ours, where the test article is unsealed and infinitely adjustable by design. Often, minor details like fabrication nuances, the decontamination effort, and the habits that pass for best practice, vary from run to run and influence the results. To counter this we adopted a detailed test plan early in the program and generally followed it during subsequent tests. Still, by the end of the program some aspects of the test were dropped as unproductive while others were expanded upon as their importance became clear. I provide the original test plan and the update used later in the program.

6K TEST PROCEDURE, DECEMBER, 1999.

INTRODUCTION

The intent of the 6K study is to obtain realistic design data for low temperature regenerators for an Oxford type Stirling cryocooler. Our test article will be a Ball 3 stage Stirling cycle mechanical cooler breadboard, modified for use at lower temperatures. Originally conceived as a refrigerator for two stages of cooling (35/60K cryocooler program), we will re-optimize it for service as a precooler for the 6 Kelvin Joule Thompson system.

Four distinct test series are planned. The first is a baseline test, where we operate the well characterized 35/60K hardware near its lowest temperatures in order to establish a performance baseline. We then conduct a lead regenerator substitution test, where we change out the coined phosphor bronze regenerator with a more suitable lead regenerator. By contrast with the baseline test data, we should be able to see the effect of the lead.

Using the design data obtained for the lead, we will then make more substantial changes to the hardware to optimize it for use as a 6K precooler. We then characterize its performance, and use this as the basis for realistic system analyses of the full system. Finally, we will experiment with alternate materials in parts of the midstage and low stage regenerators. It may be possible to enhance the performance by a judicious use of these materials.

The purpose of this test plan is to lay out a generic, standard set of tests that will facilitate inter-comparisons of performance. Each test begin with a standard worksheet to insure that all of the relevant parameters are recorded. Preconditioning, especially purging for removal of contaminants, etc., will be noted. A photograph of the cold tip will document MLI, wiring, etc.

Each test has several distinct phases. We first record the cooldown as a measure of the internal heat capacity of the unit. We then scope the behavior trends by noting how the performance changes with small changes in key variables. In this way we sense the interplay between the gross cooing and the regenerator loss. I use this information to select the right operating conditions for the load lines. I take load lines for loads on both stages. This will result in a two dimensional performance map. The load lines will be repeated at several sets of operating conditions.

Finally, I record a full set of waveforms at select operating points. This information is useful in modeling and for interpreting the measured data. These waveforms will be of compressor and displacer strokes, voltages, currents, and operating pressures.

UNIT UNDER TEST

In these tests I will use the Phase II GSFC compressor and the Ball de-mountable 3 stage displacer. The de-mountable breadboard displacer has external regenerators that can be modified, and they will be the primary variable in this study. I will use the GSFC phase ii breadboard electronics because of its handy set of monitoring circuitry.

INSTRUMENTATION

This is a short glossary of the instruments and sensors used in characterizing the cooler.

-Cryogenic temperatures are measured with Lake Shore DT470/471 diodes, using a bias current of 10 microamps. The voltages are recorded and can be converted to temperature using their standard curve 10. The repeatability is < .1K, and absolute accuracy about 1K.

-Ambient temperature is measured with a sensistor.

-Axial motion of each component is measured electronically, and is provided in the logged data set as a % of full scale, as well as in analog form during waveform capture. Full scale is either +/- 10 volts (compressor), or +/- 1 volt, displacer. The actual full scale physical displacement has to be measured independently before assembly.

-Pressure is derived from the bourdon gauge on the gas regulator. Atmospheric pressure in Boulder is typically 12 psi. Pressure waveforms are recorded with a Sensotec miniature sensor, which is calibrated against the gauge at the beginning of a run. The sensotec sensor, which has negligible volume, mounts in a small block in the transfer line.

-Both input power and heat load are recorded on Valhalla true wattmeters. Heater resistor values and lead resistances must be noted to provide corrections to the power distribution. Lead resistances are typically 5 ohms per lead, and resistors are 400 ohms. so the leads are about 1.2% of the total. About half the power in the leads ends up in the cold end, to the total error is < 1%.

-Vacuum is measured by an ion gauge. A vacuum < 1 millitorr are usually adequate for performance testing.

The phase ii electronics has a number of analog waveform outputs:

-Compressor Voltage. This converts the pwm drive to an effective AC waveform. The conversion is 2.81 volts per volt out.

-Compressor current comes from a tap between the pwm and the motor coil. The conversion is 0.96 amperes per volt out.

-Displacer Voltage is the output of the driver, and has a conversion of 1 volt/volt.

-Displacer current is the displacer drive at 0.1 amps / volt out.

CHECKLIST TO CAPTURE THE CONFIGURATION UNDER TEST

Date: NB ____,pp ____

Test engineer:_____

Purpose of test: comments:

Compressor:

Diameter		Cm
Stroke		Cm
Coil resistance	1.05	Ohms
Motor constant	12	Nt/amp

Transfer line

Length external to body	
Transfer line ID	
Pressure gauge present?	

Displacer piston
Pp stroke Y =

	Diameter	Length	Radial clearance
Shaft piston	0.7 mm	2 cm	0.45 mils
First stage			
Second stage			
Third stage			

Regenerator

	Type	Outer diameter	Inner diameter	Length	porosity	Frontal area	Hydraulic radius
1st stage warm							
1st stage cold							
2nd stage warm							
2nd stage cold							
3rd stage warm							
3rd stage cold							

Thermal mass of cold tip:
Thermal mass of middle flange.

Midstage heater =
Cold stage heater =

DETAILED TEST INSTRUCTIONS:

The work below is the minimum that will be performed in each configuration. Additional work is possible, but must be preceded by a brief description of its goal and a short test plan.

I. Cooldown

The purpose of this test is to get a measure of the expander's thermal mass and heat leak. This data will be logged in a print file on the user computer, "c:\log.prn". This has to be transferred to a file "Mdddata.prn" at the end of each test.

A. Start the cooler at standard conditions[1].
B. Record the cooldown temperature of the lower two stages versus time.
C. Allow the cooler one half hour to achieve stable bottom temperatures.

Repeat this test a second time (perhaps on the next cooldown) with an extra heat load of 0.2 watt applied to each stage as a measure of the heat lift occurring.

II. Trend study

The purpose of this section is to understand the performance trends. Data will be logged in a lab notebook and transferred to Excel for inclusion in the test report. After cooldown, deviate from standard conditions to get as cold as possible. Add heat to bring the cold tip to about 20K and explore the cooler performance.

1. Increase the compressor stroke and note changes in performance (temperatures, input power).
2. Increase the displacer stroke and note changes.
3. Add 10 lbs/in2 charge pressure and note the changes.
4. Restart the cooler at a different frequency with the original pressures and strokes.
5. Measure the performance as a function of phase angle.

Identify the best operating conditions for the load lines. The baseline test will establish a set of conditions called Baseline optimum. For subsequent cooler configurations, this will be called the best condition.

III. Take the following Load lines

The purpose of this section is to characterize the cooler. Data will be recorded in a lab notebook and transferred into Excel plots for inclusion in the test report.

1. Set the cooler in the baseline optimum conditions.
a. With the midstage at no load, warm the cold tip in steps of 0.1 watt to 0.4 watts.
b. With the midstage set to 0.2 watts, repeat the cold tip load line.
c. With the midstage set to 0.4 watts, repeat the cold tip load line.

2. For coolers other than the baseline, repeat the load line matrix for the best condition for this cooler as defined in Trend test II.6.
3. Optional: If time remains, repeat the matrix for an off-optimum point.

1. Standard conditions. Compressor stroke = 100 % (out of 106% max), displacer stroke 92% (out of 95% max), 55 degrees phase, frequency = 33 hz, and charge pressure 145 psiG.

IV. Waveform documentation

The purpose of this test is to capture key waveforms at a characteristic operating point. Waveforms will be synchronized with one another by triggering off the compressor stroke waveform. Data sets will be transferred to excel for plotting.

I. Comparison data

Measure the waveform set at the operating point defined by the Baseline optimum, with 0.2 watts on the cold tip, and 0.2 watts on the midstage. These include strokes, motor voltages and motor currents, as well as pressure if available.

II. Best condition data

For other than the baseline cooler, repeat the waveform set at the best condition with the same heat loads.

3. TEST PLAN UPDATE, MARCH, 2001

By the end of the program it became clear that we couldn't judge the effectiveness of the various regenerators by simply comparing the cryocooler performance alone. Although we had been systematic in operating at the same strokes, pressures and frequencies, we were not able to keep the mid stage temperature the same from run to run. Unfortunately, this had an effect on the performance of the last stage and was confusing our results.

Because we had been systematically recording cold stage load lines as a function of heat load on the midstage, we had enough data to interpolate to a standard midstage temperature and circumvent this problem. We were able to standardize the warm end of each regenerator to the same temperature, and the capacities at the cold tip under these conditions could be compared. We wanted to take it a step further and isolate the regenerator loss. To do this we would have to know the gross cooling, and be able to estimate and subtract off the conduction and shuttle losses. The process is depicted in Figure 18 below.

What remained to be done was to understand what the gross cooling was and how it varied with temperature. We had recorded the pV waveform for 0.2watts + .2 watts for every data set. We had to find the relationship between this pV diagram and the gross cooling, and to understand how it changed over temperature. To this end we measured Pv diagrams with different amounts of heat, up to the temperature where the temperature drop across the matrix was zero. In that case we get the gross cooling directly (it's the heater power), and we can compare that with the apparent work in the pV diagram.

The process can be visualized with the help of Figure 18. At any temperature the gross cooling is consumed by the heater power and the sum of the losses. If we can get the gross cooling via the pV diagram, and can estimate the conduction and shuttle losses, we can back out the regenerator loss.

Procedure for quantitatively determining the regenerator loss.

I. Data at baseline conditions, 33 hz, 145 psiG, 106/92,55 operating condition.

A. No load on midstage tests:

Allow the cooler to drop to the no load temperatures. Use the data acquisition to grab a pV diagram for the displacer.

Add a cold tip heat load. Use the heat load to warm the midstage in 8 steps, spanning the temperature range no load to the midstage temperature. Note that the midstage temperature drops as the cold stage warms. At each point, record the heater power, Tm, and Tc, and a displacer pV diagram.

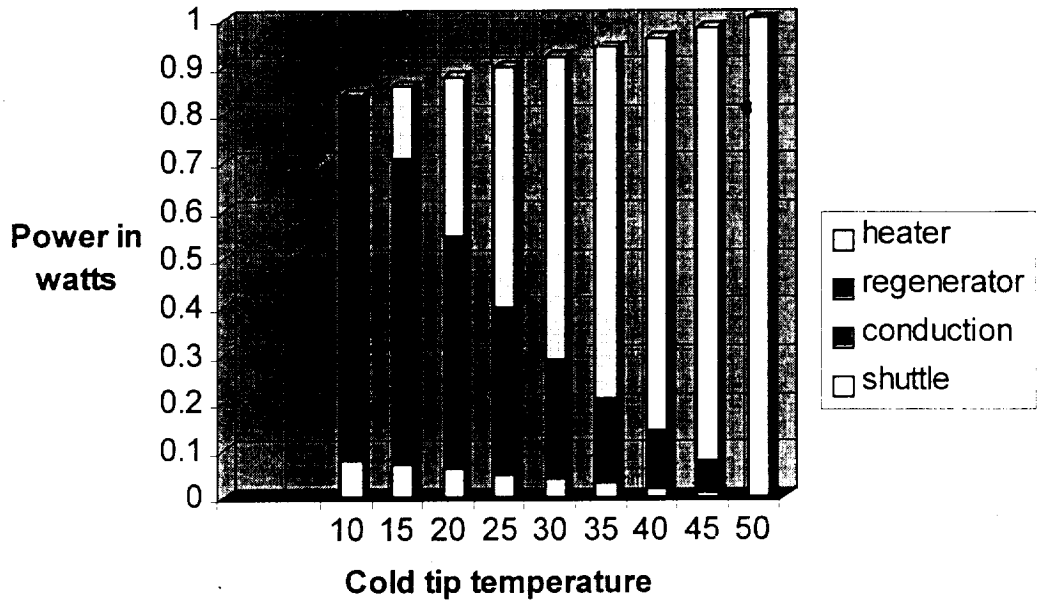

Figure 18. We can back the regenerator loss out of our data by subtracting the heater power plus shuttle and conduction losses from our gross cooling power.

Note on calibration of pV diagram:

When Tm=Tc, the losses are approximately zero and the gross cooling power is offset by the heater power almost exactly. At this point we can determine the relationship between the pV diagram and the gross cooling. The pV diagram is only approximate since the pressure is measured at room temperature, whereas we want the pressure as measured in the cold expansion chamber. We assumed that this ratio holds over the limited range of our data.

B. Repeat A with various heat loads on the midstage.

II. Data at the second "baseline" condition of 30.6 hz, 125 psiG, 106/92/55. Repeat test I at these new conditions. They will differ in their mass flow.

4. Photos of the Test setup

In the following section we document our unit under test.

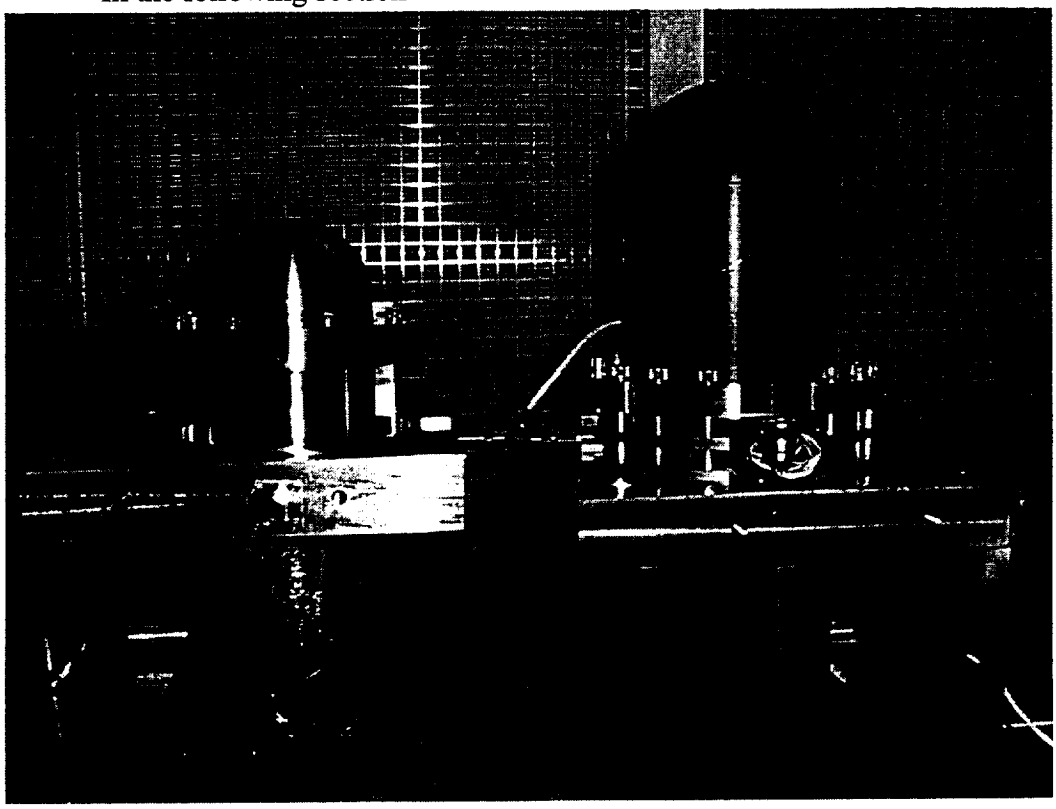

Figure 19. The 30K compressor and the breadboard displacer mounted in its test stand.

As seen in Figure 19, both compressor and displacer have bolted flanges and are sealed with o-rings, which adds flexibility but introduces the potential of gaseous contamination. Our pressure measurements were taken with the transducer located in the transfer line between the compressor and displacer. We used it to make pV indicator diagrams for both the compressor and displacer. In every experiment, at least half a dozen wraps of MLI are used to shield the coldfinger. We estimate that the radiation load on the cold tip is only 10's of milliwatts, and this load is not included in our accounting. Experiments with a polished aluminum can around part of the cold finger produced no significant improvement.

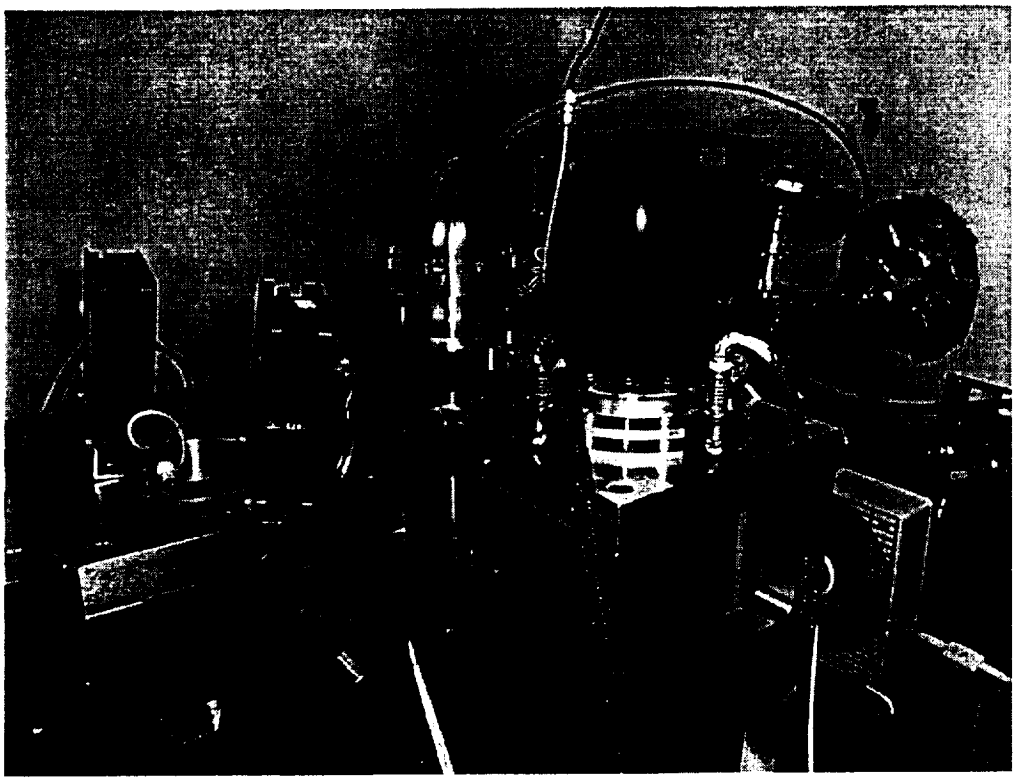

Figure 20. The cryocooler with vacuum can installed, surrounded by cooling fans.

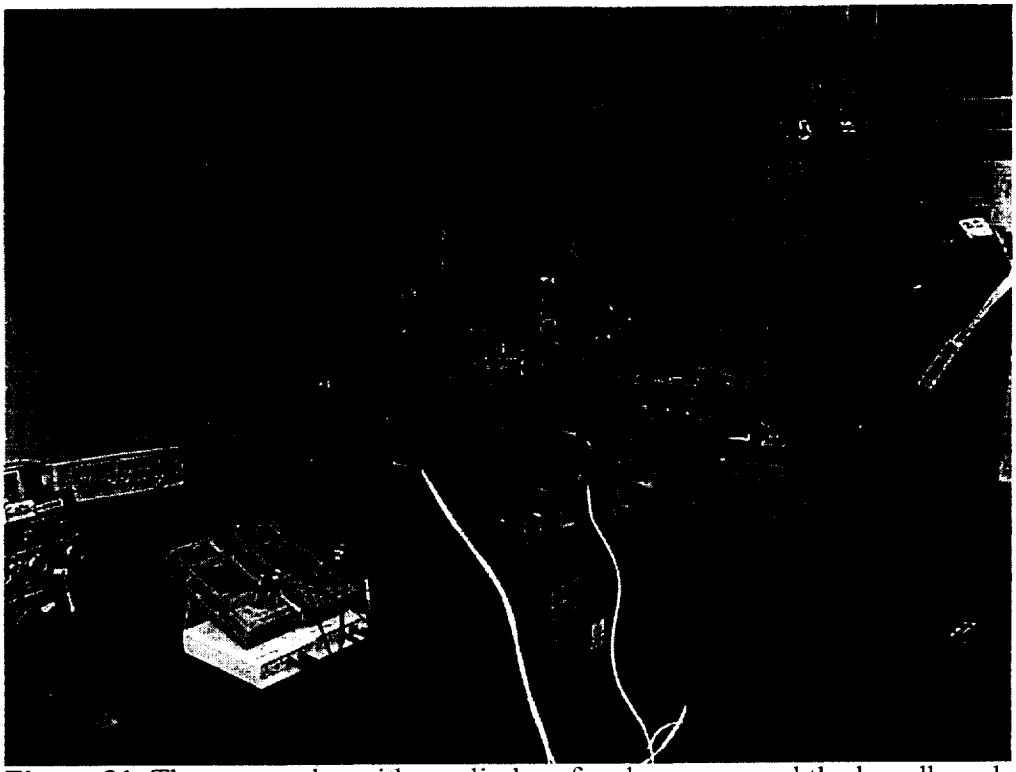

Figure 21. The cryocooler with a cylinder of make up gas and the breadboard drive electronics.

D. SPECIAL PROCEDURES

In this section we discuss two underlying technologies that had an impact on this program. The first was the use of powder regenerators. This was new to us and we describe some of our techniques and their pitfalls. The second is our method of removing the gaseous contamination from our cooler before a test. Regenerators are quickly degraded by contamination, so this was an important consideration..

1. Powder regenerators techniques

We discuss material properties, handling techniques, methods for producing the powders, and methods for loading the material into the cooler and keeping it in place.

a. Properties

In this section we discuss our three materials: lead (actually "babbit 95/5" lead antimony alloy to be precise), RE1, and REAY. Lead came with substantial baggage since it is a poison, which is unfortunate because it is cheap and effective. We begin with a list of material properties. It was important to track the weights so we could determine the porosity of our sample.

Table 2. Densities of related materials

Material	AWt	density	Sample wt	volume	Eff. Density	Porosity	vendor
RE1	167 gm	9.05 gm/cm3	11.91 gm	2.083 cc	5.72 gm/cc	0.37	University of Iowa
RE2	141	6.64	-	-	-	-	-
Lead	207	11.34	-	-	-	-	-
Antimony	122	6.618	-	-	-	-	-
95/5 (% by weight)	-	10.96	14.23	2.083	6.83	0.38	Clad metal industries
REAY (% atomic wt)	-	7.76	10.14	2.083	4.87	0.37	Atlas Scientific

Notes:
For 95/5, the fraction is weight %.
<Rho> = 1/ (ma/rhoa/(ma+mb) +mb/rhob/(ma+mb)) = 1/(x/rhoa +(1-x)/rhob)
For Reay the fraction is atomic weight %
<Rho> = 1/ (xMa/rhoa/(xMa+(1-x)Mb) + (1-x)Mb/rhob/(xMa+(1-x)Mb))

The "babbit" [Clad Metal Industries, Inc., 40-T Edison Avenue, Oakland, NJ 07436, USA]was noticeably more malleable than either the RE or the REAY alloy. This was typically not a problem and the babbit particles usually remained spherical. The babbit also had a tendency to clump during a run, presumably getting compacted by the mass flow in our machine.. They particles could also distort and thereby escape under unusual circumstances. In one extraordinary event, the particles made their way through

a screen mesh that should have confined them. In that case 4 mil particles registered perfectly with the line spacing of a 250 mesh confining screen, but should have been half again too large to fit through the opening. Apparently, because of the registry the grid was packed tight, and the extra pressure that resulted caused the particles to elongate and pop through the holes during cryocooler operation.

Once the particles got loose, they were able to flatten and thereby migrate through the clearance gaps and travel between stages. This behavior was not seen with the harder RE and REAY. Even though RE and REAY were hard, they were not found to be friable and produced no "dust" in the machine. In fact, a microscopic investigation of the debris in the cold finger's interior found more debris due to screen regenerator wire shards than dust due to the powder regenerator.

b. Health and Safety concerns

How does one decide the risk of handling lead? The chart at right shows that 10 μG of lead per deciliter of blood is a significant amount for an adult.

If a particle diameter is 125 μm, the mass of lead would be about 10μgram If you have 5L of blood, and it contained the lead in a particle, the concentration would be 2 μGram/L, or 0.2 μg Pb/dl. This is off the chart. However, lead accumulates in the body.

It probably is not a contact threat. We thought that a 125 micron sphere might become airborne, but it clearly did not. It was unlikely to be inhaled if simple precautions are taken, like using a dust mask. However, eating in an area where lead shot had been spilled would present a serious concern.

Figure 1. Effects of Inorganic lead in children and adults – lowest observable adverse effect levels

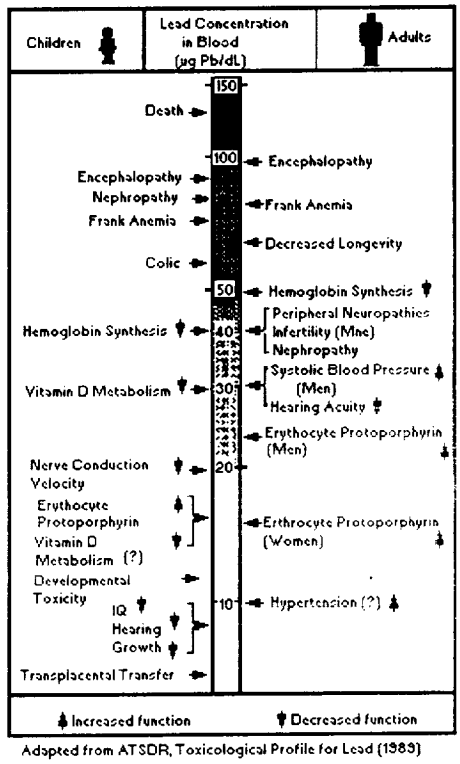

Adapted from ATSDR, Toxicological Profile for Lead (1989)

This document, prepared for Ball Health and Safety that was the controlling document for handling lead.

1. Lead procedures:

The first step is in procuring materials. Before we could take delivery of ordered material, we had to produce a document describing how we were going to handle the material in detail to Environmental Health and Safety. The plan, after negotiation, is listed below:

Introduction: Ball is under contract to do some exploratory research in cryocooler performance for NASA in the 6K program. In this 14 month program we are to modify and use existing Stirling cryocooler hardware to do the experiments, and we will deliver only data and reports. The hardware will be properly labeled to communicate that it contains lead bearing material and will remain in our possession at the end of the contract.

The problem is that I need to use lead powder in this work: A conventional means to obtain low temperatures with Stirling coolers is to use a lead shot regenerator. (Technically, Babbit, a 95% lead, 5% antimony alloy). Many of these machines are described in the literature, and almost every commercial 10K machine produced in the world uses one. I personally developed a two stage lead regenerator at Hughes in the mid 80's.

I am interested in other materials, but I believe that it is essential that our first experiment use lead since it is so widely used. Its known properties will allow me to make accurate predictions to compare with my measured performance.

An example of another material is RE1, which is produced by Prof. Karl Gschneidner at the University of Iowa. It is a proprietary material of unknown composition. It is not yet a clear alternative, either from a performance or health and safety point of view, to the lead. There may be a need to explore rare earth materials, but that will be at least a year away. If rare earth materials need to be evaluated for use, information on the materials will be submitted to EHS for review and approval, prior to purchase or receipt of sample materials.

What is the form of the lead? Unfortunately, to function properly, the lead must be in the form of fine powder, with a diameter of approximately 0.005 inches. This makes it a potential aerosol and a known health hazard. We will take the necessary precautions in the use of this material.

How much do I intend to use? The lead powder will become part of a heat exchanger within our cryocooler, which is a football-sized electromechanical machine. We will capture approximately 5 cubic centimeters of material within the cylindrical walls of the cold finger. The cryocooler is then filled with helium gas and sealed. We run the machine, and the end of the coldfinger gets cold. The lead will not be consumed. The lead powder must be constrained, or else it will migrate through the operating machinery of our cooler with obvious deleterious consequences. At the end of the testing, the unit will either be stored for future work, or opened and the lead disposed of.

Could there be a flight unit? If we are successful, we may be funded to continue with the development of a deliverable cooler with a partial lead regenerator. This would not be a consideration for several years.

Proposed assembly: Our planned assembly procedure will include redundant levels of containment to prevent even inadvertent exposure to the lead powder. We will perform the work in a glove bag, within a shot blast chamber located at Ball. The shot blast chamber is chosen because it is already an area subject to heavy metal contamination. The main concern with the chamber is reduced visibility, and special emphasis has been given to coming up with a procedure that is simple enough to do under the circumstances.

While inside the chamber, the work will be performed in a sealed "glove bag", a plastic, transparent bag with formed gloves in the wall. The regenerator, the lead supply, and hand tools will be placed within the bag, the bag will be inflated modestly with nitrogen gas, and the bag sealed with tape. The bag will be put in the chamber, and manipulated from the outside. The bag will be opened only after the lead has been transferred, and both the cooler tip and the supply container resealed.

In essence, the regenerator space is an empty tube about half an inch in diameter and a couple of inches long. Gas flows in the bottom of the tube, through the powder, and into a closed chamber on the other end. We will first insert a plug of screen mesh gauze in the base of the tube, to seal the inlet. We will spoon in powder to the desired level, and finally add a second layer of gauze, and finally the cold tip. The cold tip will mount on the end of the tube with an indium o-ring so the final sealing can be done within the bag. The lead is now captured between two filters, and the end is sealed.

At this point, the unit is sealed and will be used in our testing until we go through the process in reverse. When we are through with our tests, we will place the assembly in the glove bag. We will put the bag in the bead blast chamber, undo the indium seal, remove the top gauze wadding, decant the powder into a container, and screw on the lid. We will then pull out the lower filter, which should draw out all traces of the material from our cooler. We will then remove the components from the glove bag. I may then want to rinse the empty regenerator tube with alcohol to flush out any last traces.

Lead disposal: As outlined above, I foresee three types of contamination to get rid of.

1.) Even before we start, there are various lead powders that I am aware of, and at least a pound of fine lead wire, stashed in various places in the lab. This material predates my arrival at Ball, and I'd be happy to turn it over to you for disposal. People have brought it to my attention because of my interest in this type of cryogenics.

2.) We will provide some amount of contaminated bags, spoons, etc. in handling the material. I recommend capturing it on swaths of adhesive tape, and delivering it to you for disposal within the plastic glove bags.

3.) Bulk lead powder. At the end of our program when all future need is exhausted, we will presumably have powder to dispose of. Since this powder is regulated as a hazardous waste, this residual material must be provided to EHS in a sealed and marked container to arrange proper disposal.

2. RE, and later REAY Alloy, were not declared poisonous on the MSDS, and have a lesser degree of control. The comments below by contrast are the Health and Safety recommendations for handling them.

"After review of the material safety data sheet and other available data on Re, the following environmental, health and safety procedures must be implemented when using this material:

- Use this material under a ventilation hood;
- Avoid skin contact;
- Avoid any ignition sources;
- Collect material that comes in contact with this material (e.g., chemwipes, etc.) and dispose of as a hazardous waste.
- All material, spent or unused, must be provided to EHS for proper disposal.
- This material is considered a hazardous waste due to ignitibility.

It should also be noted that this approval is limited to the non-radioactive form of Re."

In practice, the relegation of the lead assembly effort to the shot blast chamber was onerous and next to impossible. Lead could be used in production if the program were equipped with a dedicated miniature glove box where the lead could be loaded and the unit sealed. However, we have shown that lead can be replaced by the REAY and it should be eliminated.

c. Preparing samples

The RE and Lead samples were pre-screened to size, but the REAY we had to prepare ourselves. We had to arrange for the fabrication of the alloy and its conversion to powder. We received the powder in a lot and had to grade the material. We will briefly describe each step of the process.

1. ***Production of the alloy:*** Much of this work is an outgrowth of the personal endeavors of Professor Karl Gschneidner, a materials scientist at the Materials Preparation Center, Ames Laboratory, Iowa State University, Ames, IA 50011-3020. When we decided to undertake the measurements of reay, based upon his characterization of bulk material, we contacted Prof. Gschneidner and arranged for it to be made. He has licensing arrangements with a small company, Atlas Scientific [1367 Camino Robles Way, San Jose, CA 95120] who assisted us with this procurement and split its cost. Under contract, MPC made a rod of 50 at.% x - 50% y that was 1.75"Od and 5" long. The total cost was approximately 2500$ for the fabrication of the alloy.

Production of the powder: We took advantage of a company that fabricated neodymium powder for the permanent magnet industry, Starmet Corporation. They have a process where the rod is placed in a chuck within a vacuum chamber and irradiated in some way to spawn powder. For a nominal fee (of $2500,again shared with Atlas) they converted our sample into powder. The powder was coarsely graded sent to us.

Sieving the sample:

We present the algorithm that can be used to select a sieve size to produce a sample of particles with a desired hydraulic radius.

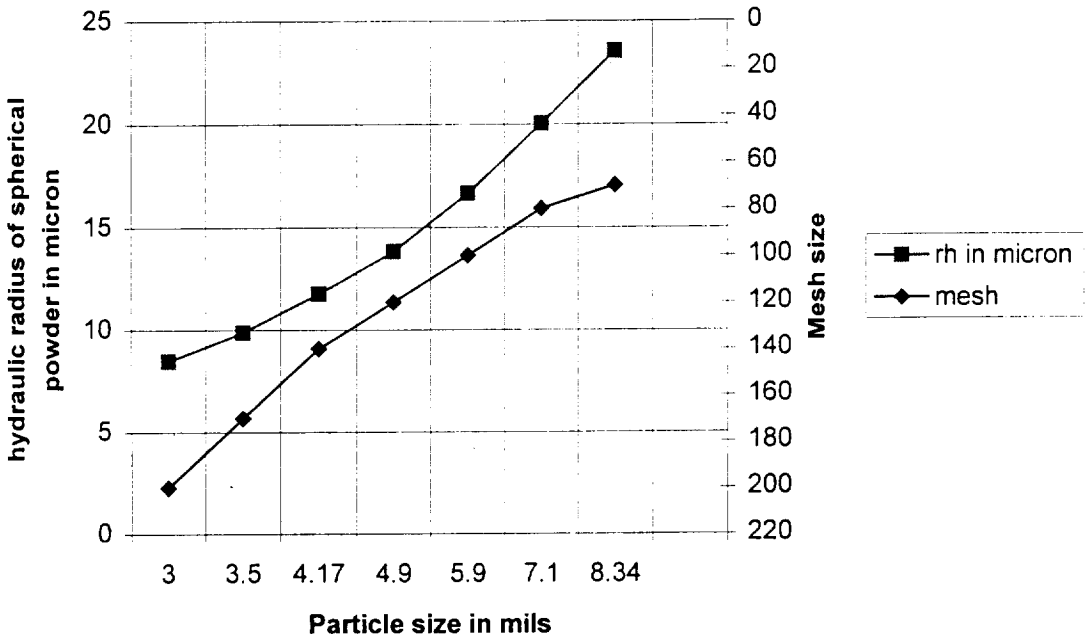

Figure 24. The figure can be used to select the sieve (in lines per inch) necessary to create a sample with a given hydraulic radius.

Imagine that the right hand axis represents a stack of sieves. A 5.9 mil particle would pass through 100 mesh sieve and sit atop the finer mesh underneath. Using rh * $A_{\perp}$ = rh*N*4 πR^2 = free volume = p* total volume =p * (N*4/3πR^3 /(1-p)) we find rh= (p/(1-p))*R/3 = 2R/3= D/9. A 5.9 mil particle has a hydraulic radius of about 14 micron.

The difficulty was in getting the "smalls" (undersized particles) to fall through the next lower screen. When we first prepared a sample we naively assumed that it would sort itself out in a single pass, ie. in a single setup consisting of hours of mechanized sifting. However, we found that approximately 20% of our first sample was smaller than the screens used to contain it, resulting in a serious particle contamination problem. In subsequent experiments we found that multiple "passes" were required, involving some agitation, but especially a brushing of the sieve. For every such "pass" the population of undersized particles was cut in half.

This suggests that the difficulty in getting the smalls to pass through was due to the occluding of the screen by the sample. A typical 2cc sample contained roughly 10^6 particles, which is enough to plug all the holes in the sieve several times. Brushing the powder back and resifting it countered this effect. Subsequent samples had half a dozen passes, and particle contamination ceased to be a problem.

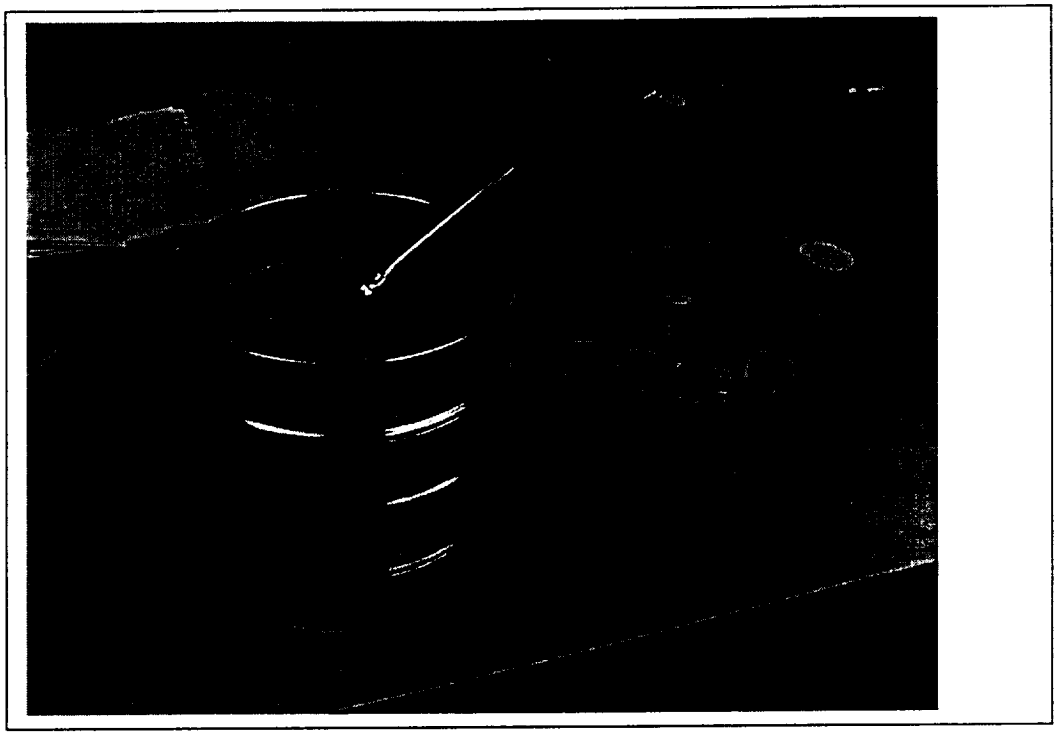

Figure 25. A partial screen stack and a collection of samples of rare earth powder. The brush is used to clean the sieve surface between passes.

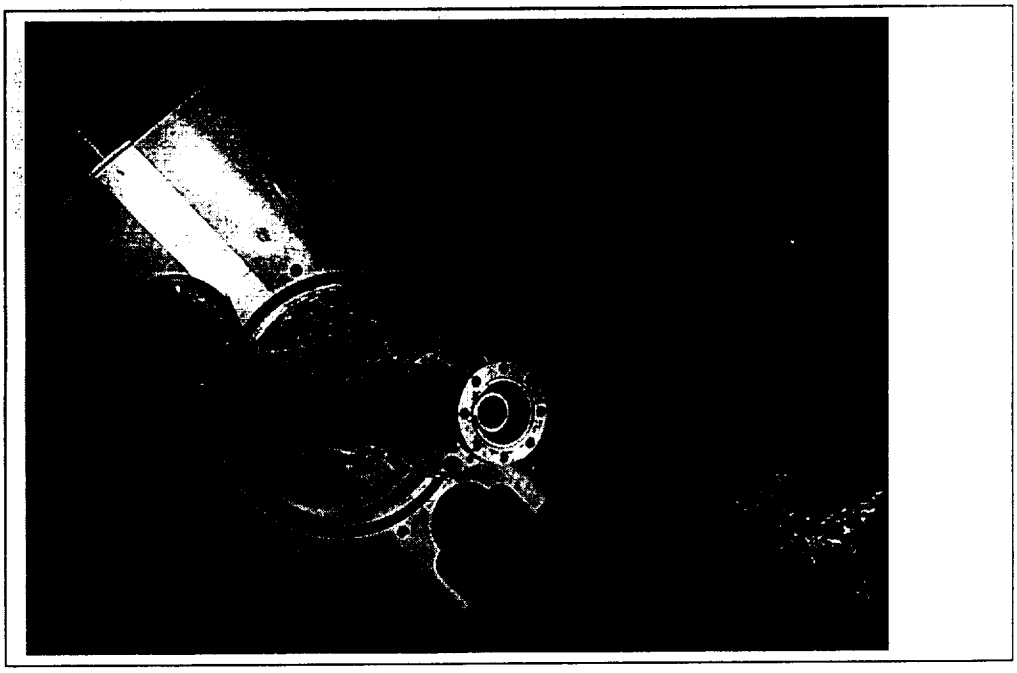

Figure 26. The regenerator material goes into the annular space between the inner tube and the outer pressure tube (flanged), shown in this end view of our cold stage.

Containing a sample in the cooler

We had to confine the regenerator material with a filter, a task complicated by the alternating gas flow in the cooler. The gas flow has to be accommodated, but meanwhile it aggressively scrubs the sample and causes the particles to exploit any flaw in its confinement. In particular, we learned that a screen *must* have an inflexible perimeter or else particles get through. We came up with the assembly shown below.

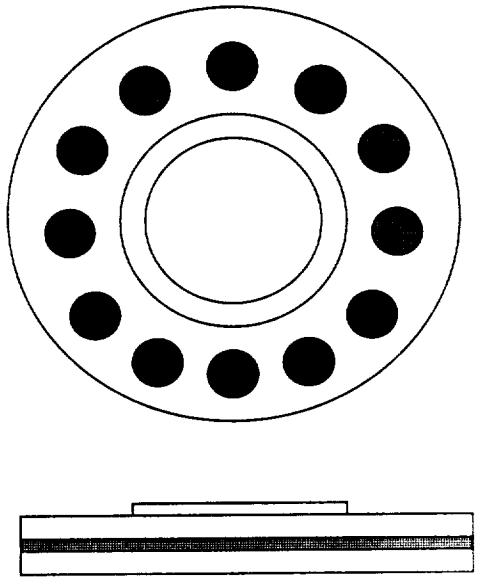

Figure 27. The filter shown at right consists of a titanium disk-hub, and a titanium washer that snap together to capture an annular, fine mesh screen.

The filter must not unduly restrict the flow of gas through the machine.

Figure 28. The sample is poured into the funnel sitting on the open end of the cooler .

We first insert a filter into the bottom of the annular space shown in Figure 26. We then add a stand pipe to the inner tube to shield the inner tube. We add a funnel onto the outer flange as shown in Figure 28 to simplify adding material. We shroud the assembly in case material is spilled. We pour powder into the funnel, and it spills into the annular region. We slightly overfill the regenerator and use a "skimming" tool to level the surface of the powder and bring it to the proper height. We close off the annular region with a second filter assembly, which is then flush with the mouth of the inner tube. We remove the stand pipe and capture the assembly with the thermal mass.

2. Gaseous contamination during lab testing

Contamination was a constant problem, especially in our low temperature range where air and even inert gases such as neon precipitate out. When we produce a deliverable cooler, we weld the unit shut and hot purge it (see Figure 29) for a substantial period of time with ultra-pure helium before sealing it permanently. We have demonstrated complete control over the unit under these circumstances. However, in these "quick and dirty" characterization tests it was impractical to treat each build like a flight cooler. Furthermore, we were constantly changing the charge pressure during the course of the experiments. As a result our test cooler was susceptible to contamination. It is therefore important to recognize and understand the symptoms, so we include here some of the characteristics that indicate when our data is suspect.

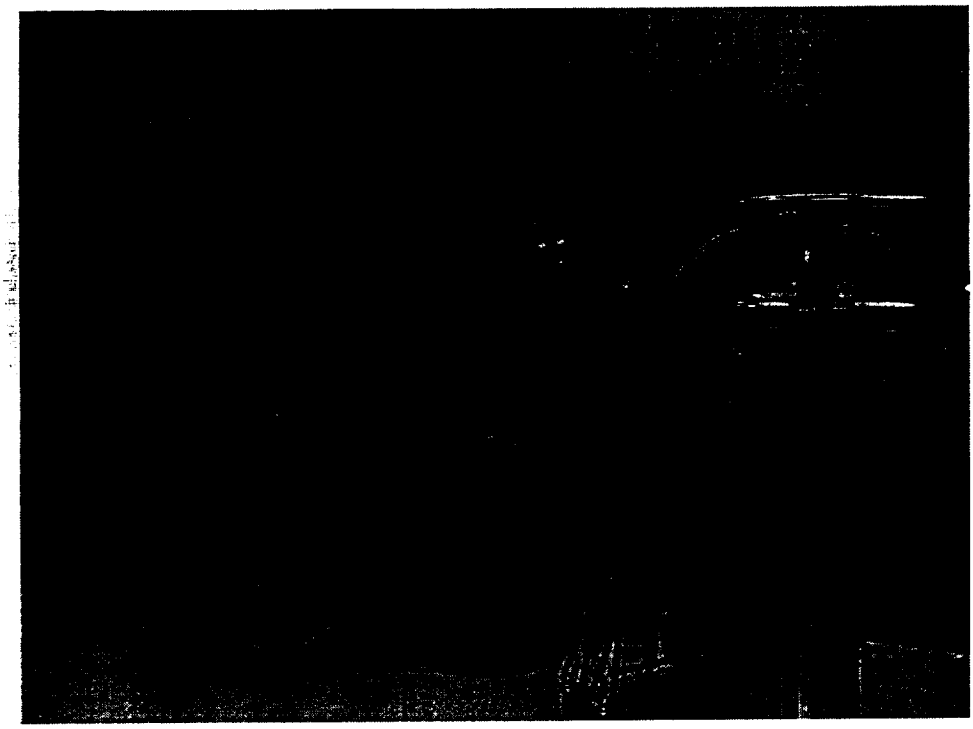

Figure 29. A hot purge station is used to process the cooler's gas charge.

The problem with an unsealed unit:

- Mistakes could be made during the extensive handling.
- Our assembly was sealed with o-rings, which admit contaminants by diffusion.
- The source gas cylinder could get contaminated through improper handling or by souring – ie., when the tank becomes contaminated internally by material coming out of the steel tank itself.
- A truncated purge schedule may not clean the internal components properly

We found that our cooler was contaminated on several occasions, and in some cases never really understood exactly why. For that reason, we had to recognize when a cooler was contaminated so we could take the appropriate steps to solve the problem. The key is that the contaminants "move", thereby changing the inner geometry during the test.

A contaminated regenerator is inefficient. There are exaggerated losses due to mass flow in the cooler even though the regenerator should be ample. It acts as if a solid chunk of contaminant blocks part of the regenerator and results in channeling. Some of the regenerator doesn't get used and it looks too small because it is only partially used.

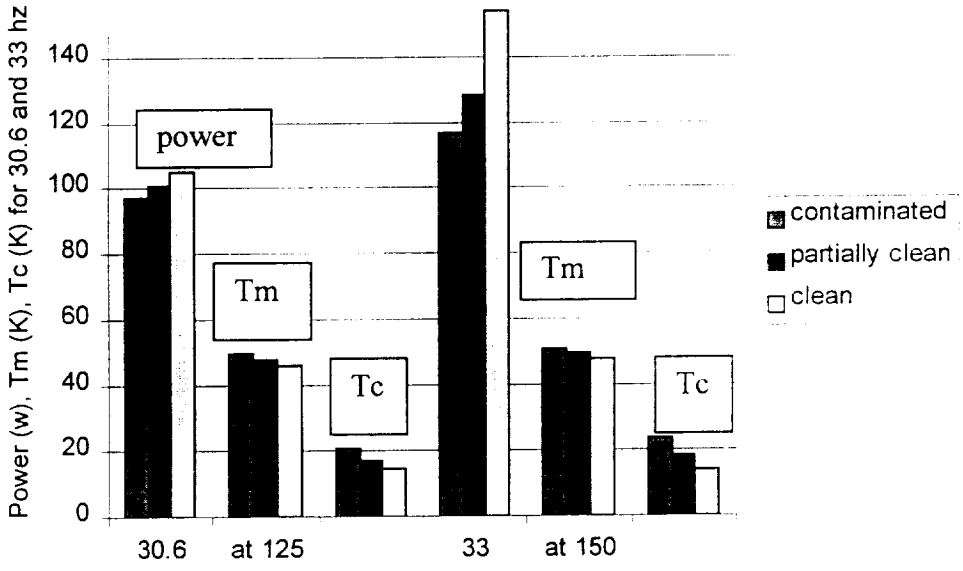

Figure 30: An illustration of several contamination trends :Power, Tm, and Tc for the coolers at 30.6hz & 125 psi on the left, and for 33 hz & 150 psi on the right. Parameters at different levels of cleanliness are compared.

There are two key observations. You lose performance by increasing mass flow when the cooler is contaminated. And this effect disappears and your results get better as you clean the unit. (The power naturally increases as it should when you clean up and get colder.)

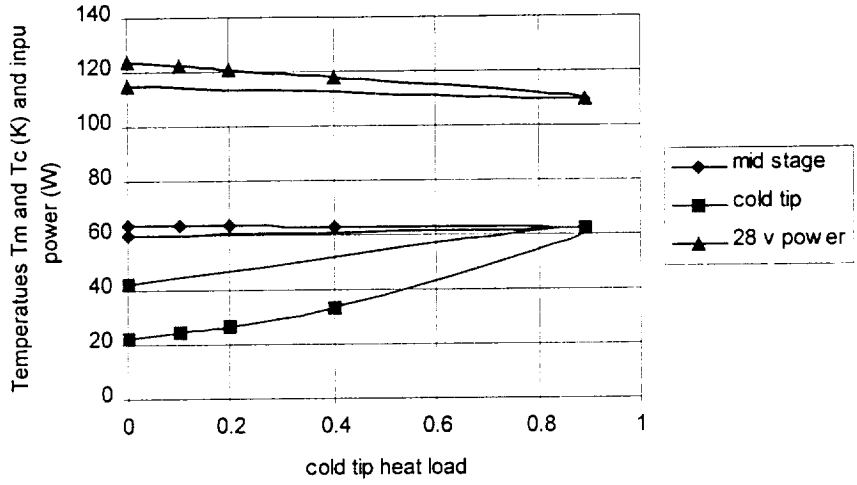

Figure 31. Hallmarks of contamination. The contamination moves around so the data does not repeat.

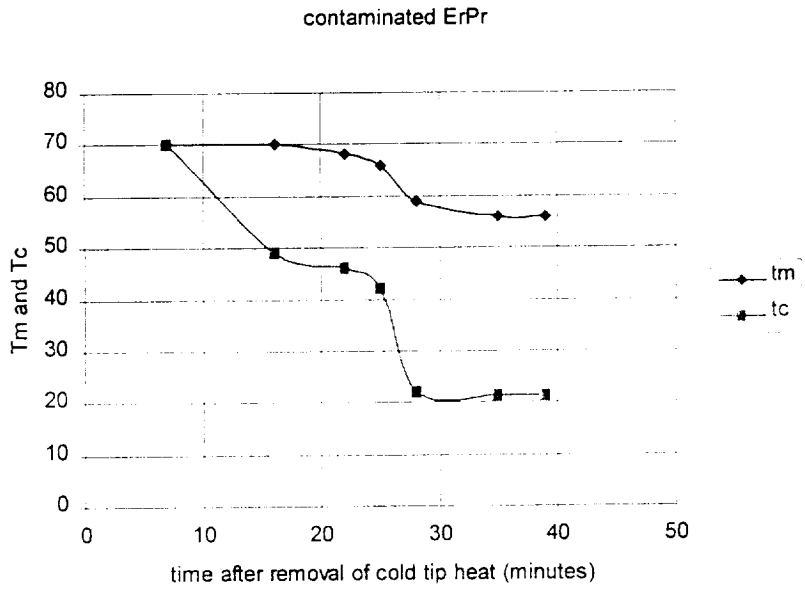

Figure 32. Hallmarks of contamination. Contamination moves around, so the performance will wander and take a long time to settle.

In this section we have tried to illustrate the clues that the cooler gives when it is contaminated. This lets us avoid including compromised data into our comparisons. These figures, taken from unsatisfactory 6K experiments, have been shown here to illustrate the contamination problem.

D. Results

Overview

In this section we highlight the key results of the program.

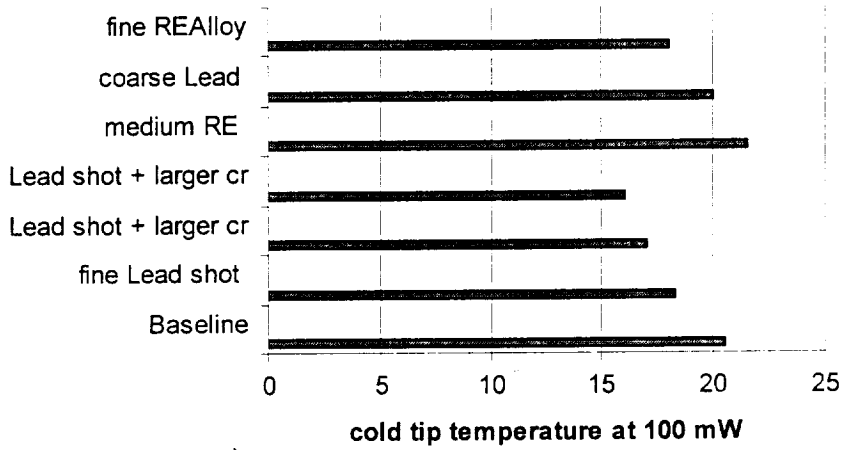

Figure 32. A single index of the performance of various cooler configurations showing the progress towards lower temperatures.

At first our configuration changes resulted in lower temperatures, but that came to a halt when we were simply substituting rare earth materials for lead in the same regenerator chamber.

A complete set of data from our best configuration, Test3, Lead shot + larger compressor:

In this section we provide a complete set of raw data in our best configuration with lead shot and the larger compressor. We measured load lines per the test plan at three frequencies, 30.6, 33, and 35.5 hz. The first set is best below 17K, the last is best above 22K, indicating how the low temperature region is qualitatively different as the regenerator becomes ever more important. For all sets the cooler was operated at 106% (ie. "full") compressor stroke, 92% displacer stroke, and 55 degrees phase angle.

Table A. The performance data at 30.58 Hz and 121 psiG.

Watts on		0 w midstage		0.2 w midstage			0.4 watts midstage		
Coldtip	pwr	Tm	Tc	Pwr	Tm	tc	pwr	tm	tc
	watts	K	K	W	K	K	w	K	K
0	115	45	14.7	115.7	48.5	14.8	115.2	51.7	15.8
0.1	114	45.12	16.5	112.8	48.5	17.1	112.6	51.7	18
0.2	111	45	19.1	110.4	48.1	19.7	110.6	51.4	20.8
0.4	107	44.3	26.2	106.6	47	27.2	105.3	50.3	29

The data is plotted in Figure 34. The cold tip load line shows that we are carrying 100 mW at 16K. The load line shifts up in temperature as we apply extra heat to the midstage. As the midstage warms, it leads to a higher pressure ratio, but reduced indirect cooling at the midstage, resulting in the slight drop in temperature seen.

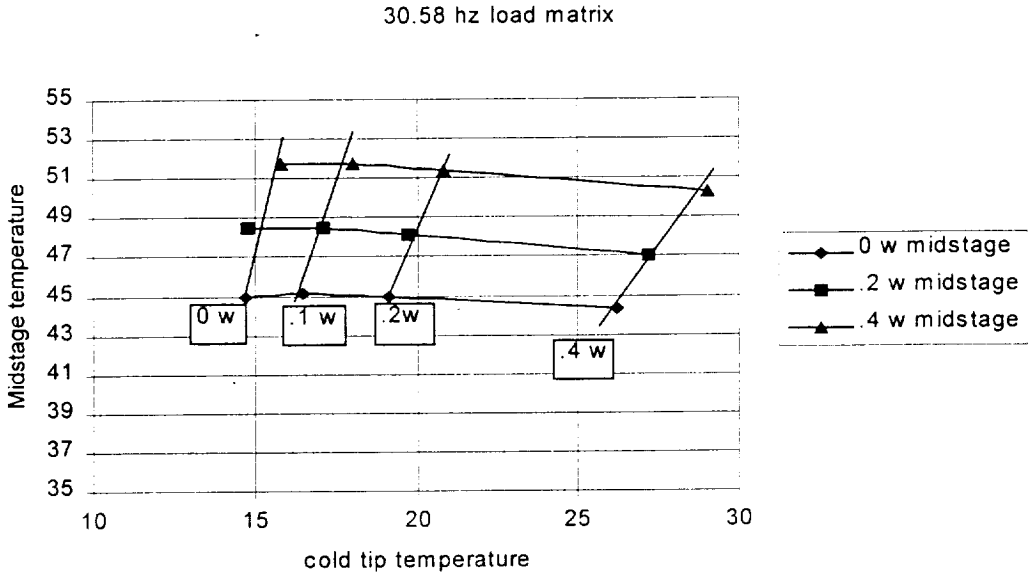

Figure 34. The load line matrix for 121 psig, 30.58 hz, with 106, 92, 55 degrees parameters for the cooler. This is much improved over test 2b.

Table B. Performance data at 33.08 Hz, 145 psiG.

Watts on	0 w midstage			0.2 w midstage			0.4 w midstage		
Coldtip	Pwr	tm	Tc	Pwr	tm	tc	pwr	tm	tc
0	152	48.2	15.3	154.2	49.6	16	154.12	52	16.3
0.1	151.5	48	17	152.3	49.8	17.4	151.6	52.2	17.8
0.2	149.6	48	18.7	149.4	50.1	19.2	148.9	52.1	19.6
0.4	145.6	47.1	22.9	144.3	49.7	23.7	143.9	51.8	24.2

The operating conditions for this set were those that had been optimum for the original 35/60K cooler, so they were really not the best for this cooler working at its lowest temperatures. The data is plotted in Figure 35 below. The midstage load line is considerably stiffer, rising just 4K instead of 6K as it had in the 30.58 hz case.

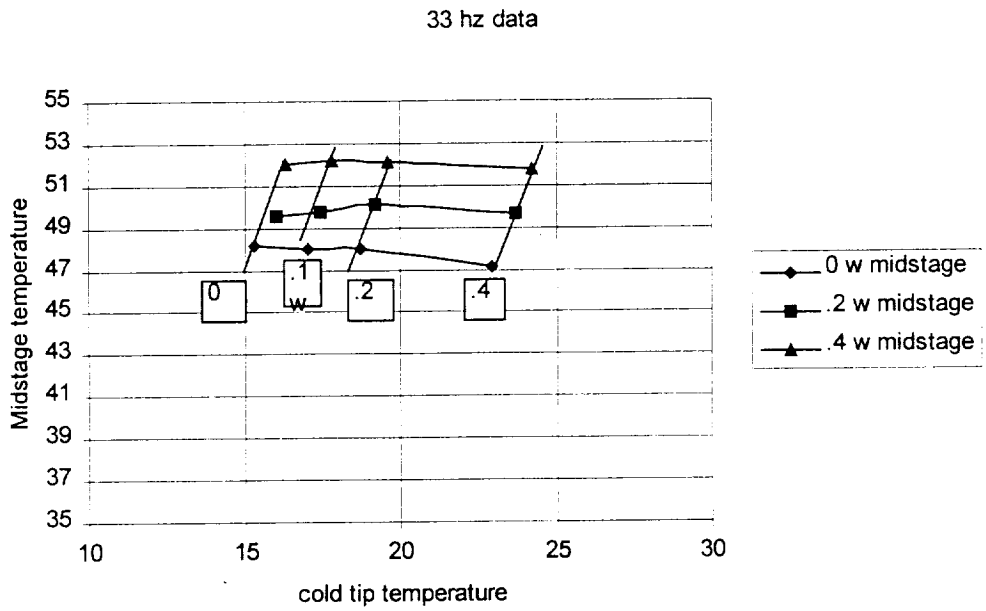

Figure 35. The load line data at 33 hz and 145 psig. The midstage no loads higher (48K), but has a stiffer load line. The cold tip also no loads >15K, but the capacity at 20K is about a quarter watt, perhaps 30mW higher than the 30.58 hz case.

Table C. The loadlines for the cooler at 35.5 Hz, and 121 psiG charge pressure.

Cold tip	0 watts midstage heat			0.2 watts midstage heat			0.4 watts midstage heat		
Watts	Pwr	Tmid	Tc	Pwr	Tmid	Tc	pwr	Tmid	Tc
	W	K	K	W	K	K	W	K	K
0	124.3	47.2	14.8	122.4	49.4	15.3	120.4	52	15.7
0.1	122.6	46.8	16.8	120	49.2	17.3	118.4	52	17.9
0.2	119.7	46.5	19	118.2	49	19.4	115.6	51.7	20.3
0.4	114.9	45.3	24.3	114.3	48	25.5	112.6	50.6	26.5

This data set was taken to contrast with the 30.58 hz data. It has the same charge pressure but is at a higher frequency. Surprisingly, the cold tip gets almost as cold and cools better at 0.4 watts. This shows that the performance is frequency sensitive, but that frequency is not yet a dominating parameter.

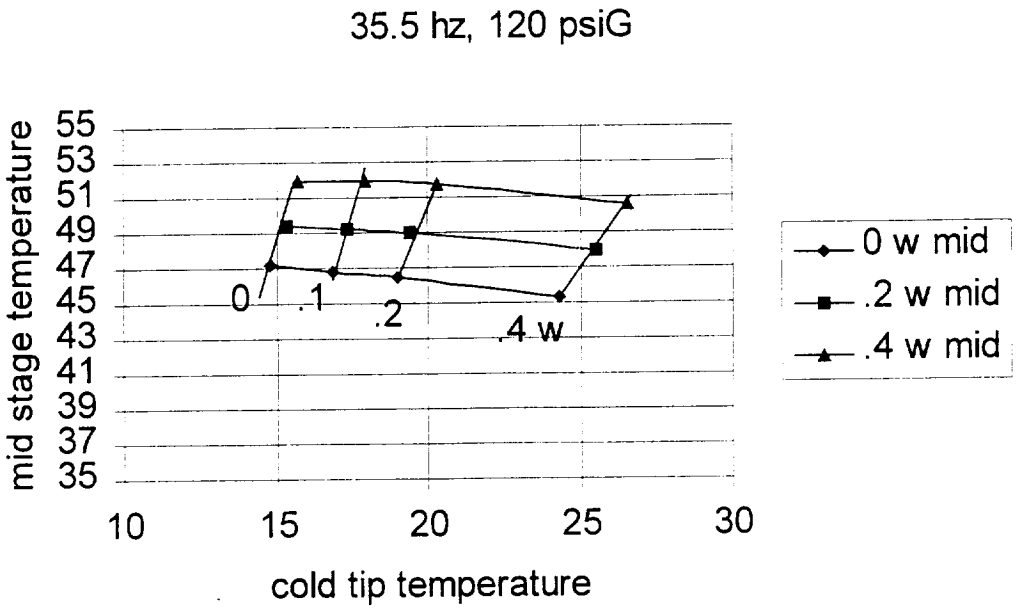

Figure 36. The cooler still no loads below 15K at 35.5 hz, so its low temperature performance is not seriously offset by frequency. It holds 24K at .4 watts, rather than the 27 K at lower frequency.

As a final comment, we point out that we were able to achieve this level of performance on two separate occasions, which suggests that it is a true, repeatable behavior. Following our Test 3, we reconfigured the cooler with rare earth RE in the midstage with disastrous results as seen in Figure 32. Before going any further we re-built the Test 3 configuration with new materials and were able to repeat this performance in detail.

Test 1 Essential result

The essential result in test 1 was to de-rate the actual pressure ratio in the cooler, thereby lowering the predicted amount of gross cooling at any temperature. This is one of the factors in the overconfidence in our predictions in Figure 14. In this test we had resurrected the original 35/60K cooler and characterized it at lower temperatures. We compared measured and calculated waveforms and tried to resolve the discrepancies.

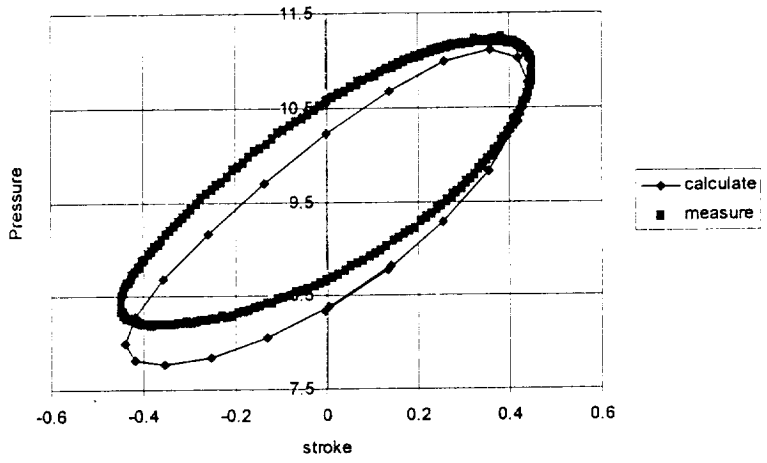

Figure 37. A waveform comparison suggests that 2 cc's are missing in the math model.

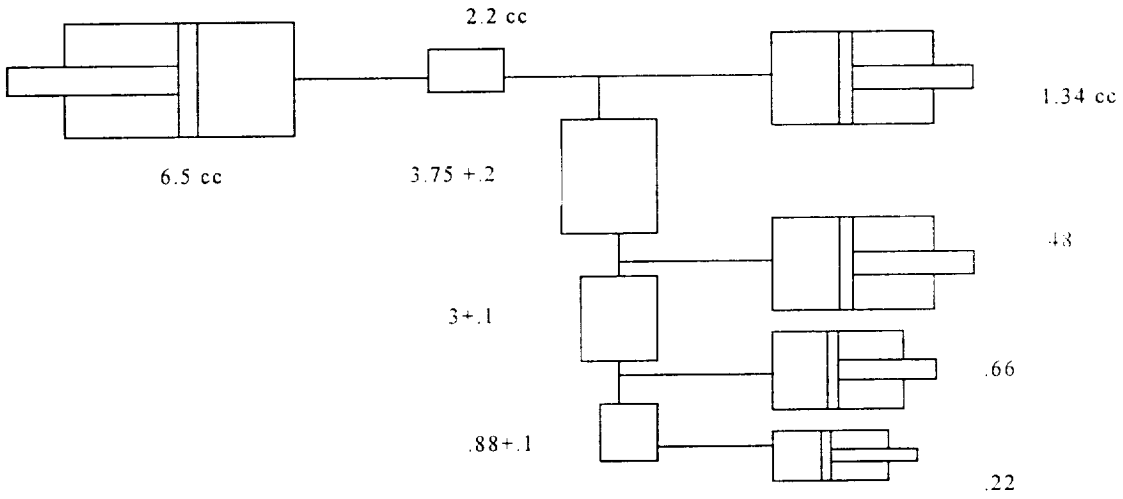

Figure 38. The original volume model, putting the missing 2cc's in perspective.

We knew we had to add dead volume to get the pressure ratio right, but the question was where to put it. It turns out that the predicted cooling capacity is sensitive to where the extra volume was added. We found that by adding .2cc at ambient, .3cc at 180K, .1cc at 45K, and .05cc at 20K, we remained consistent with the measured cooling capacity at the 3 stages. A year later, we discovered that these volumes were explained by the fact that our screens were more porous than we originally thought.

Test 2's essential result is that lead alone is not the answer.

We introduced lead into the coldfinger in test 2. We simply wanted to see the effect of the material, so we designed the regenerator to otherwise resemble the original screens in terms of dead volume and pressure drop. We compensated for the lower porosity of balls relative to screen by making the regenerator bigger, and we did this by increasing the area and not the length to keep the frontal free area pAf about right. Finally, we chose the ball size so we would have about the same surface area between the material and the gas.

Table 6. Properties of the original screen and subsequent lead ball regenerators.

	test 1 regenerator	test 2 regenerator
Material	phosphor bronze	lead (95:5 PbSb shot)
frontal area = Af	0.62 cm2	1.01 cm2
length = L	2.4 cm	2.26 cm
free area = pAf	.36 cm2	.39 cm2
Porosity = p	.58	.4
dead volume = Af*L	.86 cm3	.91 cm3
Hydraulic radius = rh	.same	same

How about Pressure drop $dP = f\,(L/r_h)^* G^2/2^*rho$?

- f goes as c/Nr, and the c for balls (44) is about twice that for screens (24)
- G= mdot/pAf and Nr are about the same for both
- => f and dP for the lead regenerator will be 1.8x the screen regenerator
- small part of the overall pressure drop in the cold head.

How about the regenerator loss? The heat leak goes as $1-\varepsilon = (1/Ntu,0)^*(1/(1-cmin/cr))$

- $Ntu,0 = .5^* Nst * L/rh$
- $NstPr^{2/3} = .09\ f$ for screens (K&L)
- $NstPr^{2/3} = .06\ f$ for balls (K&L) "detailed interpretation of static data"

So, 0th order regenerator performance about the same except for the matrix material capacity via Cr.

By design the main performance improvement would be due to the superior heat capacity in the lead shot. Both materials had adequate thermal penetration depths. Our models predicted a +300 mW at the cold tip, accompanied by a -300 mW *loss* of cooling at the midstage since we simply were removing a heat leak between them. Judging from the Test 1 results, this meant 47K at the midstage and 300 mW at 18K.

We found the shift to 47K at the midstage, but gained only 100 mW at 18K at the cold tip. The discrepancy suggests a complicating factor, which we now think is an extra loss in the *upper* stage regenerator which added to its heat leak at the same time we were removing indirect cooling by the stage below. The higher temperatures made the cooler look worse than it was.

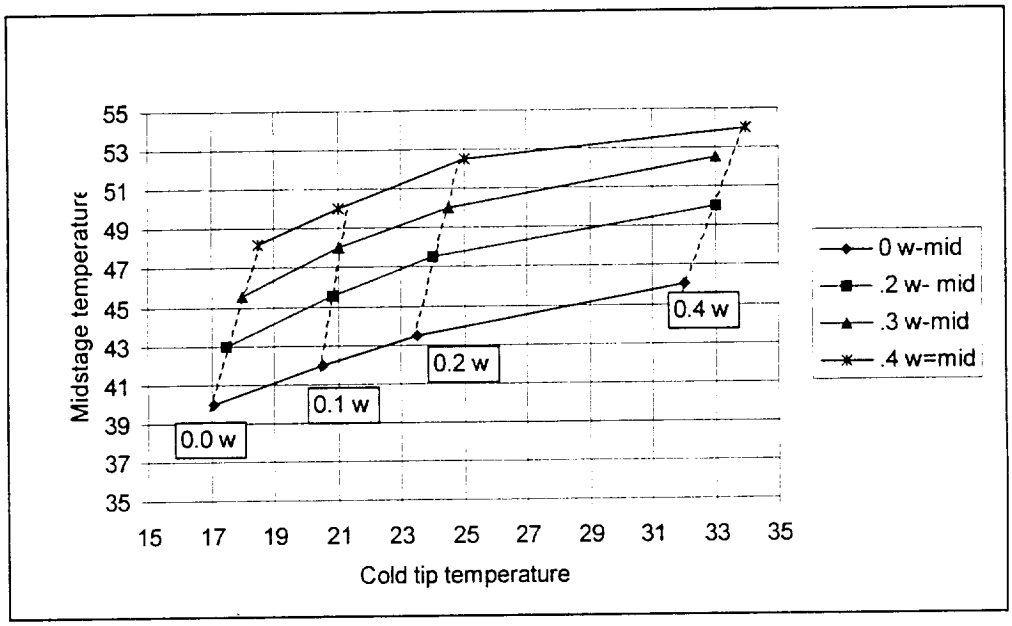

Figure 40. Test 1 Figure 7, Dec2299.doc. The performance of the 35/60K cooler with phosphor bronze screens at baseline conditions.

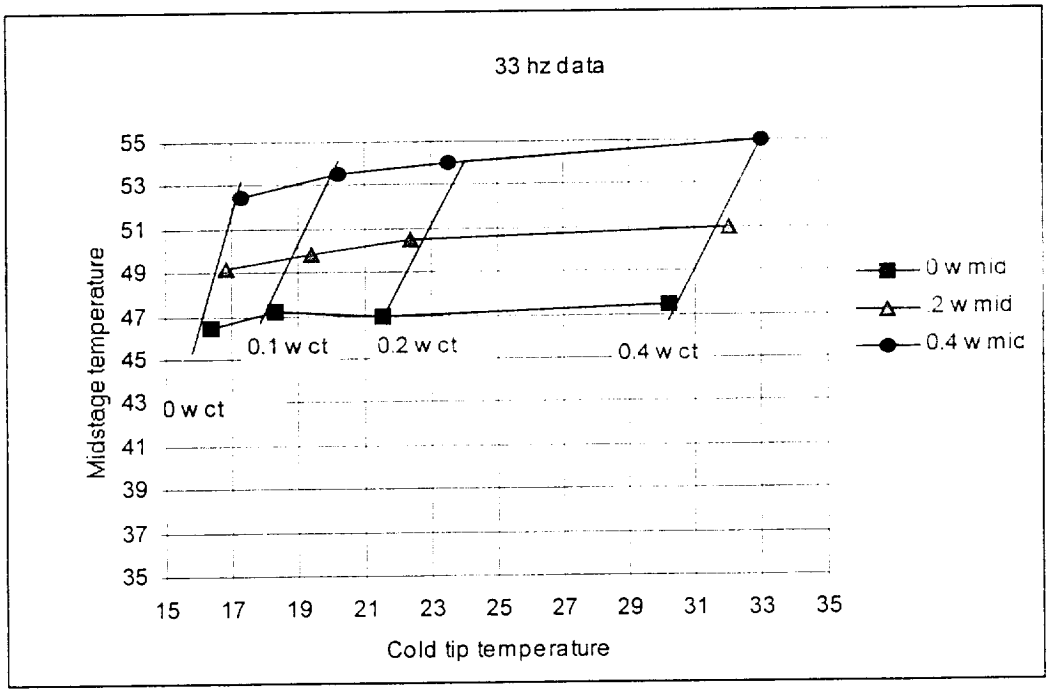

Figure 41. Test2, Mar2100.doc. The performance of the same cooler with an "equivalent" lead regenerator shows modest improvement.

Test 2 and Test 3 Frequency dependence

It is clear that a fundamental driver in our experiment is our high operating speed. One of our auxiliary experiments was to see how important frequency was. There are many reasons to expect trouble at higher frequencies: less time to transport heat from the gas to the matrix, less time for heat to penetrate the matrix, and less equilibrium time for the expansion itself

In this test we kept the operating conditions and the pressure the same, and, disregarding resonance conditions, drove the cooler at lower and lower frequencies to see how it would affect the net cooling.

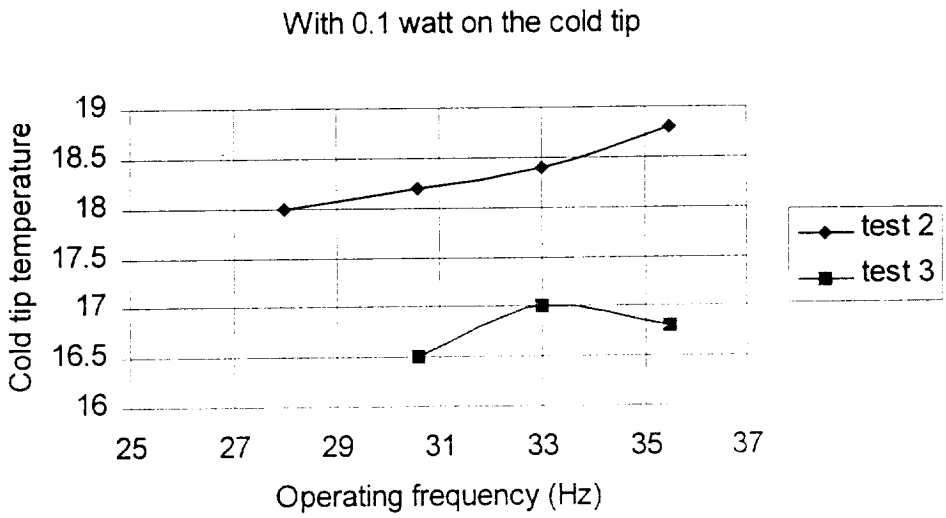

Figure 42. In both experiments, operating frequency alone was not a major factor in achieving low temperatures, although it always helped.

In our limited range of experience, the cooler frequency has not yet become a major parameter. However, real gas effects come on strongly below 15K and will sap the gross cooling power through the effects described.

Test 3 Key results

It was obvious during the test 2 results that we were limited by the displacement from the compressor.

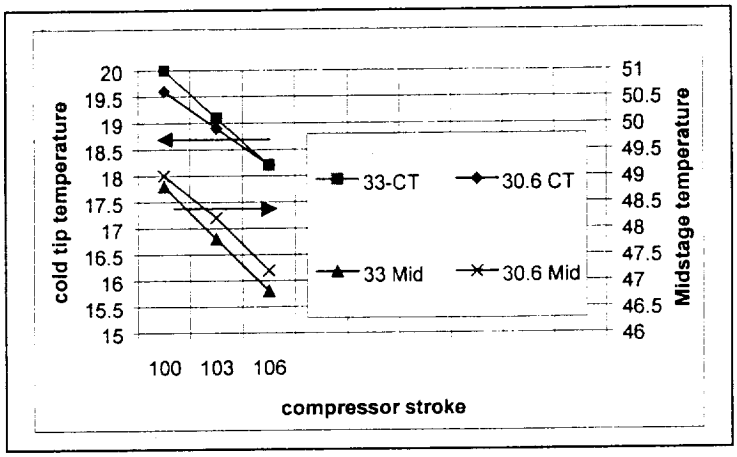

Figure 43. In test 2, both the cold tip and midstage temperatures responded to compressor stroke.

The solution was to increase its displacement. We fabricated new piston/cylinder sets, increasing the diameter from 2.15 cm to 2.44 cm, the largest the old hardware would permit.

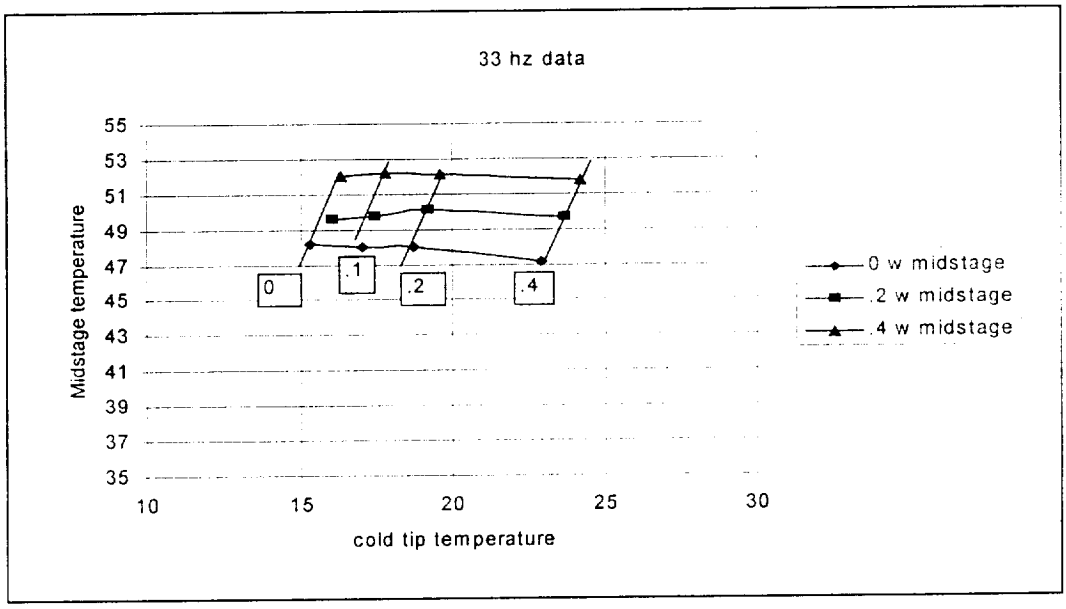

Figure 44. In comparison with Figure 41, from Test 2, we find that the extra displacement has significantly helped the cold tip performance.

We now achieved nearly 200 mW at 18K. The full data set has been provided earlier in this section. Test 3 trend data showed that the cold tip responded to more compressor stroke, suggesting even more improvement in this direction. However, the midstage was saturated, indicating that this stage also could be better optimized to support the lower temperatures.

Test 4 essential results

This set of tests were unproductive and time consuming. We list here the principal efforts.

- An attempt to trick the compressor into greater strokes failed. This was an electronic control problem that would be hard to circumvent.
- A radiation shield at 40K to "protect" the cold tip had no effect
- A cooler configuration with RE shot filling the last 20 % of the midstage did not cool well at all. The problem was most likely a flow restriction due to the kind of filter (Figure 27) we could squeeze into the tight annular geometry at the midstage rather than a problem with RE itself.

Test 5

As discussed during the introduction to test 2, we had gone to great length to keep the surface area between tests the same so we could clearly see the effect of lead. In this test we set out to contrast two lead regenerators with different amounts of surface area.

In Test 3 we had characterized fine lead shot. In Test 5 we set out to characterize both very fine and coarse lead shot, and then move on to evaluate our medium sample of er. By measuring the size effect with lead, we would be able to factor size out and get a better feeling for the difference between the materials.

We were able to successfully characterize the coarse lead but not the very fine lead. When we attempted to characterize a very fine lead regenerator, a number of particles escaped and contaminated the cold head. This led to a complete tear down and refurbishment of the displacer.

In any case, we were able to characterize lead in two different sizes, and at several different speeds. The results are in qualitative agreement with expectations, and even agree quantitatively with the predictions of REGEN3.1. In all, a confirmation of our overall approach.

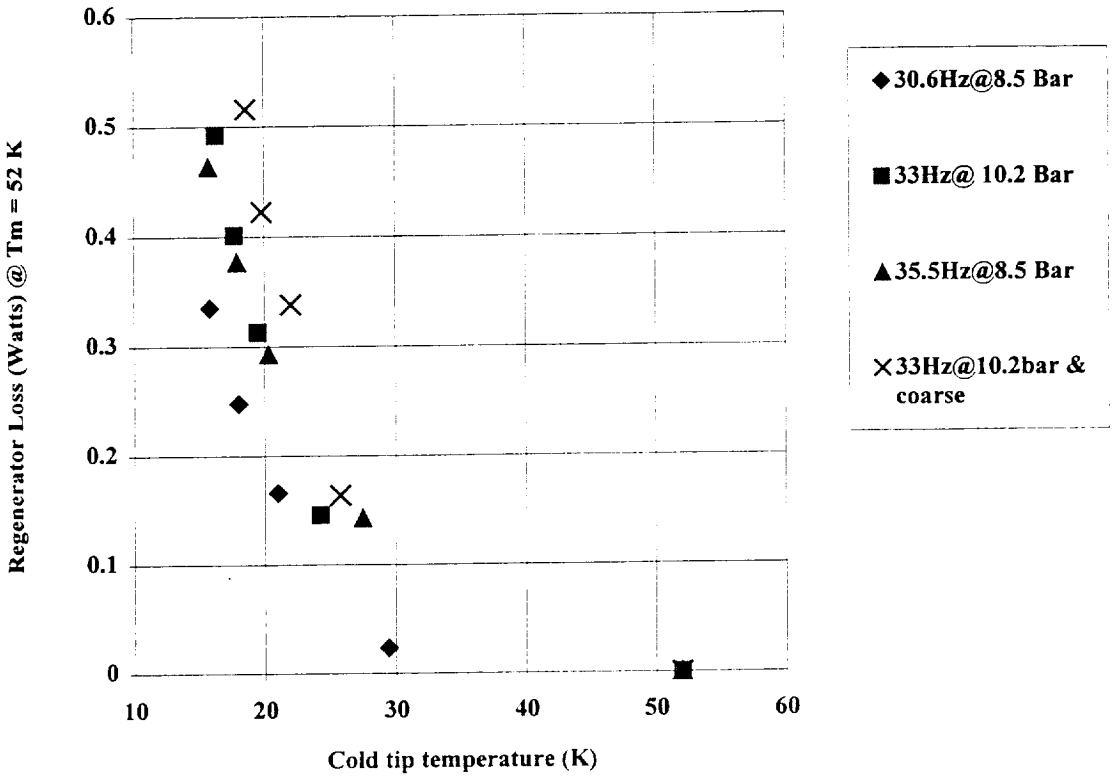

Figure 45. The experimental results for fine and coarse 95/5 Lead-Antimony shot show expected behavior patterns.

This data has been compiled from the load line matrices, calculations of the conduction losses, and measurements of the gross cooling capacity, as discussed in the approach section. In each case the data matrix has been interpolated to fix the warm end of the regenerator at 52 K to allow an inter comparison of results. The results fall qualitatively in the right order:

- The {30.6hz &8.5 bar} to {33hz &10.2 bar} comparison shows that the loss increases with mass flow brought about by pressure and frequency.
- Similarly, the {30.6hz & 8.5 bar } and {35.5 hz & 8.5 bar} comparison shows that the loss increases with mass flow brought about by frequency alone.
- The {33&10.2 bar & fine} and {33 & 10.2 Bar & coarse} shows that the coarse powder, with less surface area, has a higher regenerator loss as expected.
- The results for {33 Hz & 10.2 bar} and (35.5 Hz & 8.5 bar} are close, because they have a very similar mass flow.

We modeled these individual cases using the NIST program REGEN3.1. The results are shown below.

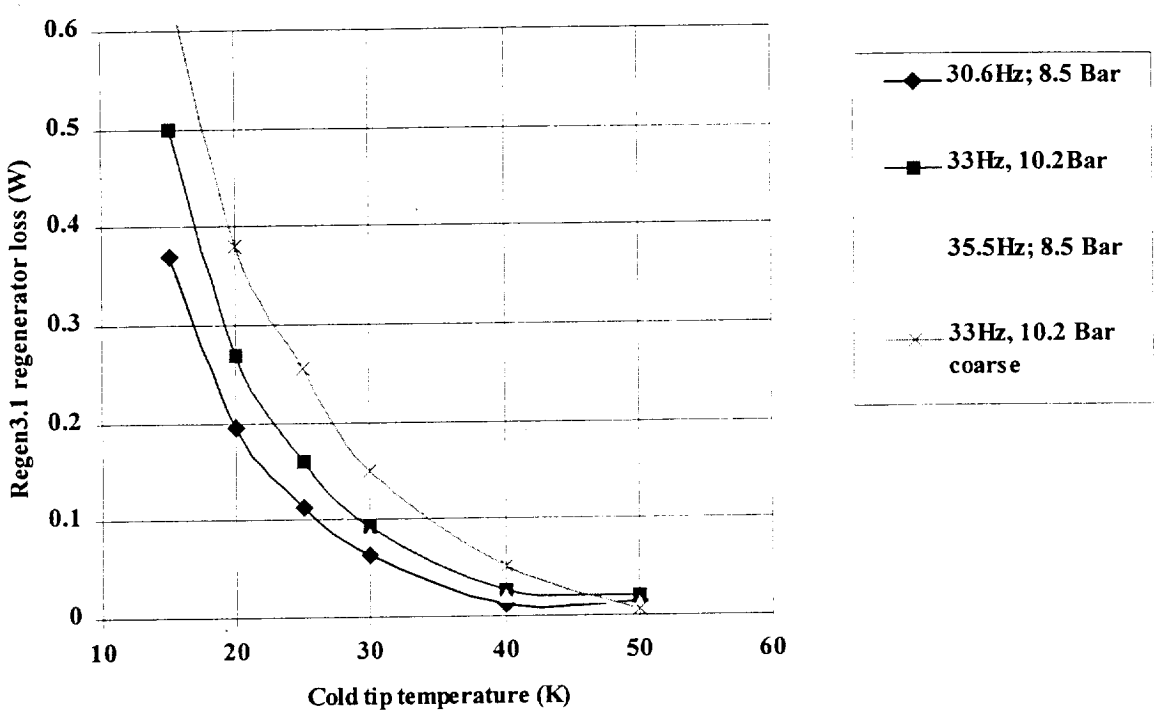

Figure 46. REGEN3.1's predictions for the regenerator loss agree in detail with each case considered experimentally above.

This agreement validates both our modified method of interpreting our data, and the predictive ability of REGEN3.1. Although we characterized RE in test 5, we defer the discussion until the next section, where we add the newly formulated REay into the mix.

Test 6 Introduction of Rare earth alloy REAY

After some delay resulting from the contamination and rebuild of the hardware, we characterized fine REAY according to the revised test plan. Part of the effort involved characterizing the gross cooling over temperature. We learned that we had to de-rate the room temperature displacer pV diagram by a small factor (12%) to make it agree with our direct thermal characterization of the gross cooling. Once this factor was established, we could use the pV diagrams from earlier data sets to arrive at the gross cooling in each case.

The results for REAY are shown along with those of lead (95/5) and RE below. We have chosen to group the data by their common operating conditions. In Figure 47 we show the results at low mass flow (30.6 hz and 125 psi charge pressure), and in Figure 48 we show the results at high mass flow (33 hz and 150 psi charge pressure). Other than the regenerator material and particle size, all conditions were the same for each set. Again, data for each material is interpolated to a start temperature of 52K.

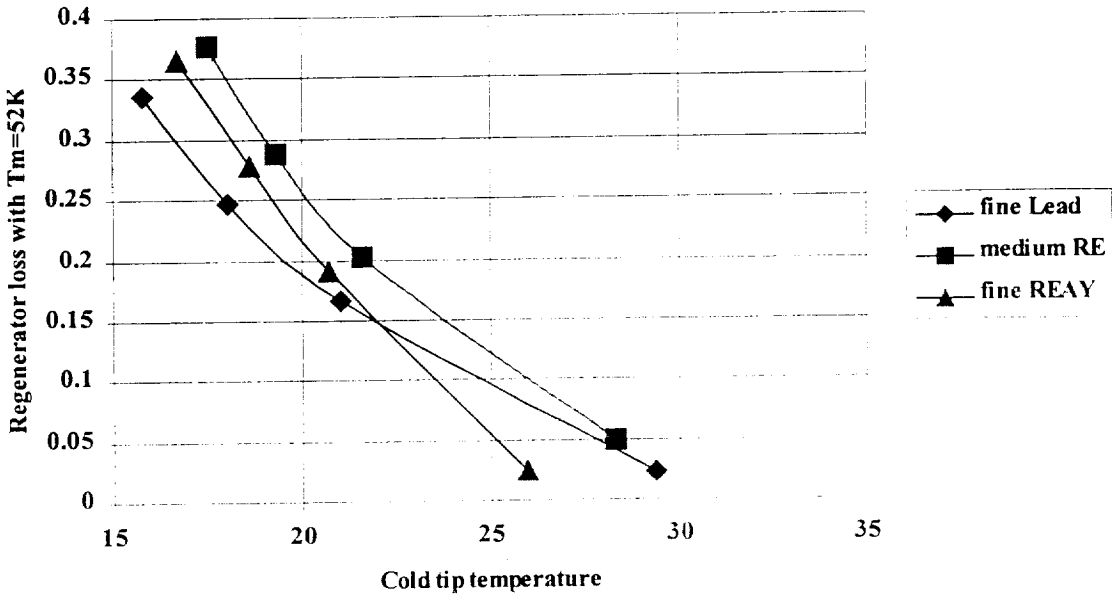

Figure 47. An inter comparison at low mass flow conditions at 30.6 hz, and 8.5 Bar. Lead and REAY are similar, although lead seems to have an edge.

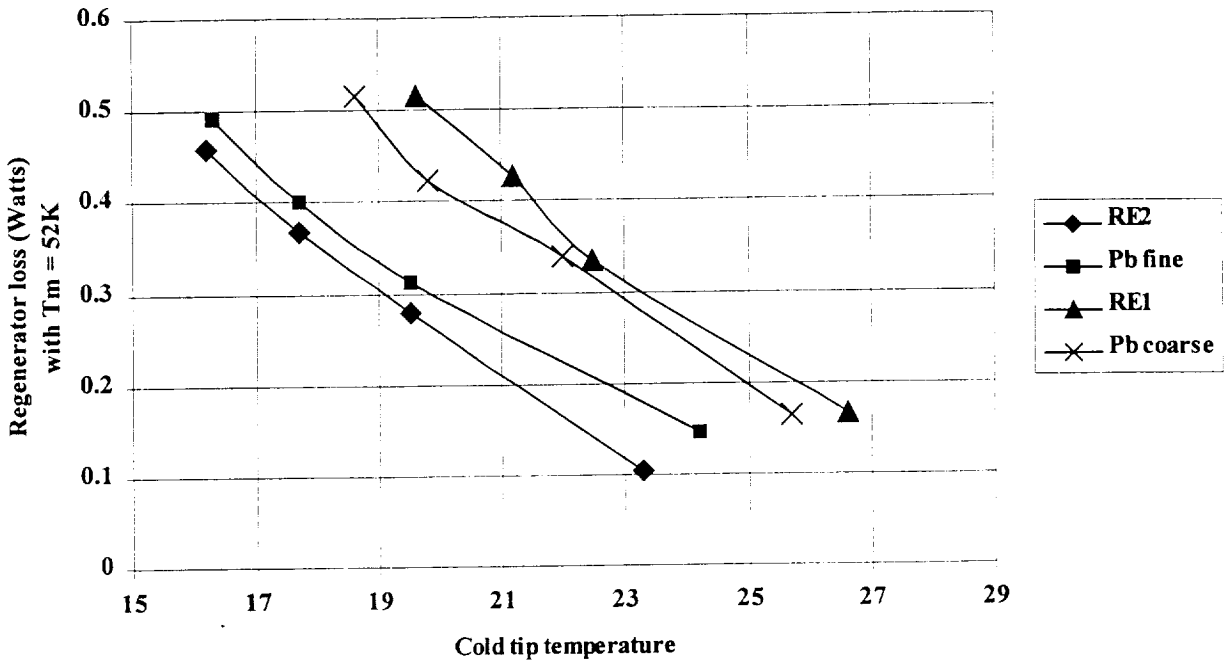

Figure 48. A comparison of regenerator loss for RE (Rare Earth #1), lead, and REAY (RE2) at 33 Hz and 10.2 Bar. In this case REAY is best.

Judging from the last two figures, RE seems to be slightly worse even after accounting for its relatively large particle size. REAY and lead have taken turns providing the best performance, so in our opinion REAY seems to be an adequate substitute for lead, at least in this temperature range.

Summary

In this section we outline how we would design a low temperature precooler based upon what we have learned. We have seen how profound the regenerator loss becomes at low temperatures, so the recommendations by in large are strategies to minimize this loss. We note that our work here provides quantitative design data for a precooler operating in the 15-16 K temperature range, adequate for precooling a reasonable JT stage. But our work most likely falls short of being sufficient to design a 10K Stirling cooler. Real Gas effects, primarily the enthalpy dump and regenerator imbalance, set in strongly below 15K and will sap an already heavily loaded regenerator. Our conservative goal here is to design a practical 15K precooler.

1. Employ an even larger compressor. In this program we adapted existing hardware, increasing the diameter size as much as we dared. In a new program, this limitation would not exist, and would enable us to move further into the realm of lower pressures and higher pressure ratios.

2. Lower the midstage temperature. There is no reason not to re-arrange the 3 stage cooler to better adapt it for use at the lowest temperatures. What we have now was optimized for use in IR systems requiring multiple stages of cooling. As our data indicates, the losses still are proportional to the temperature drop across the regenerator, so dropping Tm will be beneficial. Ultimately, there is a point where loss terms not proportional to the temperature difference will dominate, but this definitely is not the case in our cooler.

3. Use graded regenerators, i.e., load the lower end of the stage with finer particles than you currently used. Our regenerators are limited to a certain degree of coarseness because of the need to keep the pressure drop down because of the parallel clearance gap. For a uniform ball regenerator, the majority of the pressure drop occurs at the warm end. This means that one can pack finer powders in the lower half and not influence the total pressure drop significantly.

4. Investigate densified sintered compacts of REAY. I envision thin washers of sintered REAY materials used at the end of the cold regenerator.

   The leading concern with a sintered mass is the enormous increase in thermal conductivity, so to start we assume that the powders are sintered in thin the form of thin washers that can be stacked. The discontinuity between layers provides the necessary thermal isolation.

   The technical advantage of densification would be the reduction in free volume within the sinter. The drop would be due primarily to a decrease in hydraulic radius, and secondarily to a decrease in surface area as particles melt together. Now, the pressure drop will scale as $(L/pA_f r_h^2)\ (\eta/\rho)$ mdot, and the regenerator loss will scale as (r_h^2) mdot/(pAfL) *(1-cmin/Cr). For a given macroscopic geometry, the pressure drop will go up, but so will the thermal contact to the material and the ratio of material to helium, which will help with regenerator limitations. The additional benefit is the elimination of cold dead volume, which unloads all of the upper regenerators as less mass flow is required to feed it.

   A practical benefit may be that the sintered compacts act as the low temperature particle filters if they have sufficient integrity. At present, with my titanium filters, I get no benefit from the body of the filter since it has negligible capacity and negligible heat transfer area.

Part II. 6 K Hybrid cryocooler design

A. Hybrid Cooler Definition

It is our goal to design a hybrid cryocooler that can provide 100 mW of refrigeration at 6K. The JT cooler and the Stirling precooler are intertwined, and we need the parameters of one to define the other. During the last several years we have experimented with materials and configurations to learn how to design a practical precooler. We have settled on a 14K temperature at the low end because we think that we can build a precooler capable of lifting several hundred milliwatts at that temperature, based upon our lab testing. This is the information sought in our studies, and this will be the starting assumption for our 6K cooler precooler. We now embark on the definition of the 6 K cooler and design a JT system to meet the requirements. Once it is defined we can analyze its components to arrive at the thermal loads that a precooler must carry to allow it to work. We begin with a very brief discussion of the parts of a hybrid cooler and their key attributes.

Table 49. Key components of a 6 K hybrid cooler.

Item	Function	Requirement
6 K interface/exchanger	Connect to instrument	Contact area, rigidity, vibration isolation
JT valve	Provide expansion	Impedance; resistance to blockage
45-14 K exchanger	Absorb the 100 mW out of the fluid	De-couple stages
14 K heat sink	Dump dH to precooler	Equal temperatures to .1K
40K-14K exchanger	Isolate 14K from stream	99% efficient, compact
40K heat sink	Sink 40K streams	Temperatures equal to 1K
180K-40Kexchanger	Isolate 40K from stream	99% efficient, compact
180K heat sink	Sink 180K streams	Temperatures equal to 1K
Stirling displacer	Provide precooling	Inefficiencies + conduction + radiation
180K baffle	Shroud & protect insides	Assume e=.2
40K baffle	"	"
Vacuum can	For testing only	Allow system to be tested
Stirling compressor	Drive displacer	Sized for thermal load
Rotary compressor	Provide flow, Rp	40 mg/sec at Rp =2, Ph/Pl = 6/3 bar
Filter	Particulates & gaseous	Protect cold head
Sensors	Monitor Stirling/JT points	Test data, control loop feedback
Control electronics, Stirling	Provide drive waveforms, control	Existing E200 or derivative
Control electronics, JT	Provide rotary drive	MPC corporation motor driver

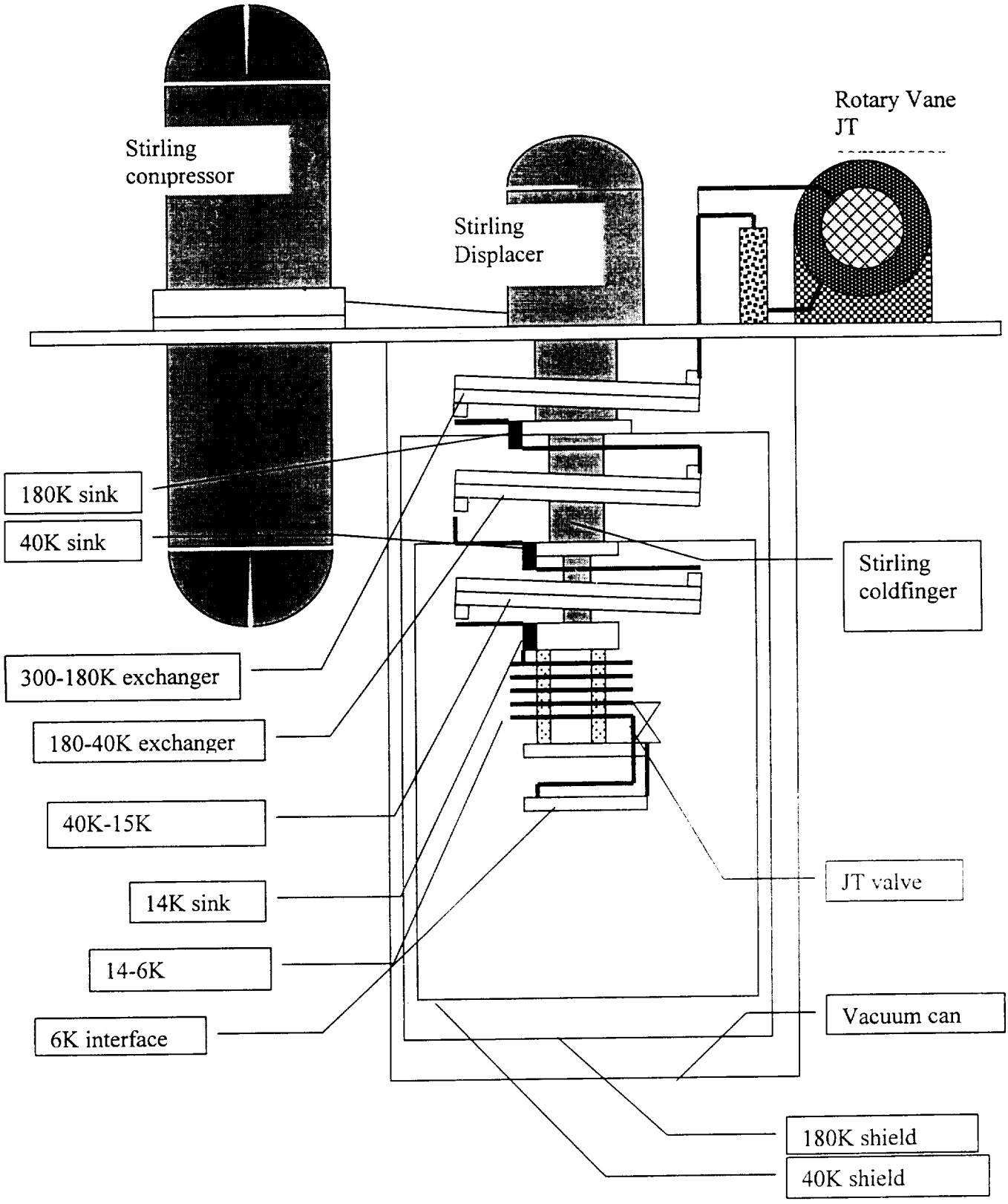

Figure 50. A diagram illustrating the parts of a Hybrid cooler.

B. JT Cooler Sizing

1. Basic thermodynamic trade study for the JT cooler

We will perform a simplified sizing of a 100 mW 6K cryocooler system. We will rough out the design of our JT cooler, and determine its precooler requirements. We will estimate loads from radiation and mechanical support. We will size a Stirling precooler to handle these loads. We will arrive at the size, mass, and power required to provide 100 mW of cooling at 6K.

We configure the JT cooler along the lines of one developed on an earlier Ball program for a 10K cooler. We accept the basic pump design, and simply scale its size and operating pressure. However, we do take a minute to consider whether 3He would be of any advantage at 6K. After optimizing the design, we derive values of pressure and mass flow that are the inputs to later, more detailed considerations.

Thermodynamic model for the JT refrigeration available at 6K.

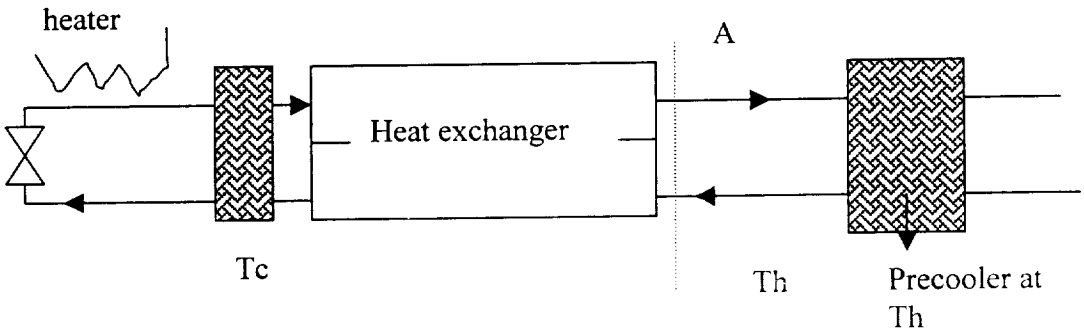

Figure 51. The amount of refrigeration we estimate at 6K can be deduced with the help of this simple model of a precooler, heat exchanger, and valve.

Basic model:

The easiest way to see the refrigeration available at the cold tip is to put a control volume around the cold tip after the precooler node. The fluid has inlet and outlet streams penetrating the control volume at A. We assume that both streams have the same temperature Th. Of course, the inlet stream can be thermalized to Th by the precooler, but we must assume that the outlet stream is the "minimum capacity" stream of the system and therefore adjusts its temperature to Th also.

Consider the enthalpy current through the surface at A. There is an enthalpy transport out of the surface A:

$$Hdot = mdot * [H(Pl,Th) - H(Ph,Th)]$$

since the inward flowing high pressure enthalpy is less than that of the outward flowing low pressure enthalpy. In order for refrigeration to occur the precooler has to sink this enthalpy current. To conserve energy in the control volume heat has to be added at the valve.

Control volume model including the ineffectiveness of the heat exchanger:

Consider an inefficient heat exchanger between the precooler and the JT valve. It will diminish the heat lift at the cold tip by its ineffectiveness. To understand how this comes about, first assume that the fluids are balanced and that the exchanger is ideal. The fluid moves through, exchanging heat with itself perfectly, and the enthalpy current at the entrance A pops out on the other side of the JT valve.

More realistically, the regenerator is imbalanced. The outlet stream can't completely pre-cool the inlet stream. There is internal heat exchange, but the low capacity, low pressure side cannot absorb all the enthalpy exuded by the high pressure side as it enters. So the high pressure side is at a temperature above Tc when it leaves the heat exchanger.

Enthalpy has to be conserved in the isolated heat exchanger, so the high pressure side exhausts at some temperature Tx > Tc such that

$$\text{Mdot}\,[H(Pl,Th)-H(Ph,Th)] = \text{Mdot}^*[\,(H(Pl,Tc) - H(Ph,Tx)]$$

Just as before, the enthalpy current at the cold end of the exchanger is the same one that occurs at A. When we allow that our heat exchanger is inefficient, some heat isn't transferred from the entering to the exiting stream, and we have to add that as an extra heat leak to Tc. The expression we use is (from Kays & London, Compact Heat Exchangers)

$$Q_{leak} = \dot{M} C_p(T_{h,out} - T_{c,in}) = \dot{m}^*[H(P_h, T_h) - H(P_h, T_c)]^* (1 - (C_c/C_h) * \varepsilon)$$

Where $\varepsilon = [\,1 - e\{-Ntu(1-C_c/C_h)\}] / [\,1 - (C_c/C_h)e\{-Ntu(1-C_c/C_h)\}]$

Following K&L, Cc is the capacity of the cold, low pressure exhast stream, and Ch is the capacity of the warm, high pressure incoming stream.

$C_c = dH(Pl)/dT = \{H(Pl,Th)-H(Pl,Tc)\}/(Th-Tc)$
$C_h = dH(Ph)/dT = \{H(Ph,Th)-H(Ph,Tc)\}/(Th-Tc)$

In the limit of high efficiency, the heat leak expression reduces to the excess enthalpy delivered *at Tc*, which means that it includes the heat that has to be extracted to drop the incoming stream from temperature Tx *to Tc*. Once cooled to Tc, the fluid provides refrigeration at Tc of

$$\text{Mdot}^*(\,H(Ph,Tc) - H(Pl,Tc))$$

In fact, the heat leak has in fact to be subtracted from this gross cooling in order to arrive at the net cooling. The net cooling is to be 100 mW.

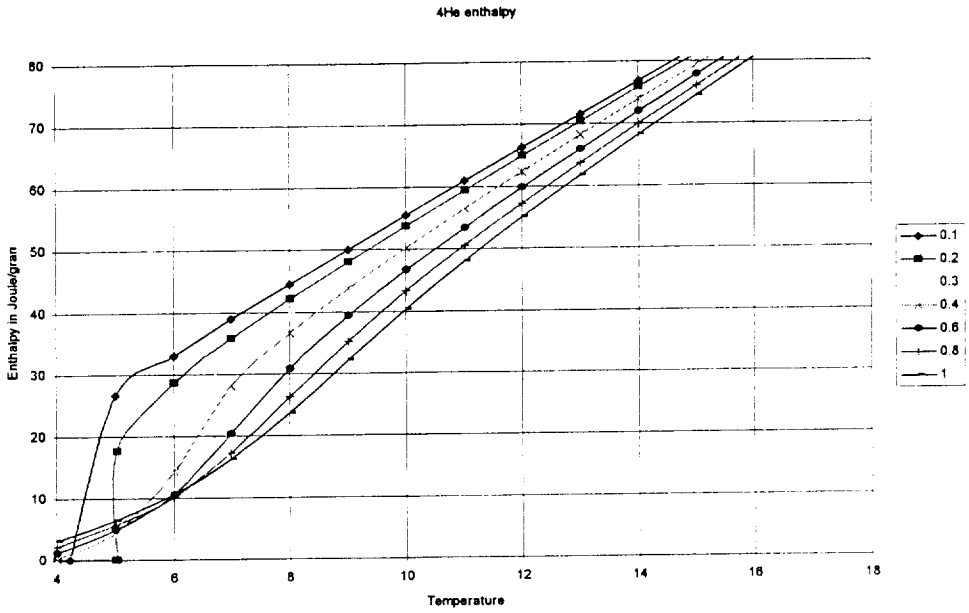

Figure 52. Helium 4 enthalpy from 4-16K and 1-10 atmospheres. The legend is in Mpa.

We plot the ^{4}He enthalpy in Figure 52. We have confined the thermodynamic properties to this range because they correspond to the possible operating conditions for our Rotary vane cooler. The enthalpy drops below the simple 5/2 RT value characteristic of an ideal gas because of the enhanced compressibility above the critical point. Note that at 6 K the enthalpy is completely depressed at 6 Bar and above.

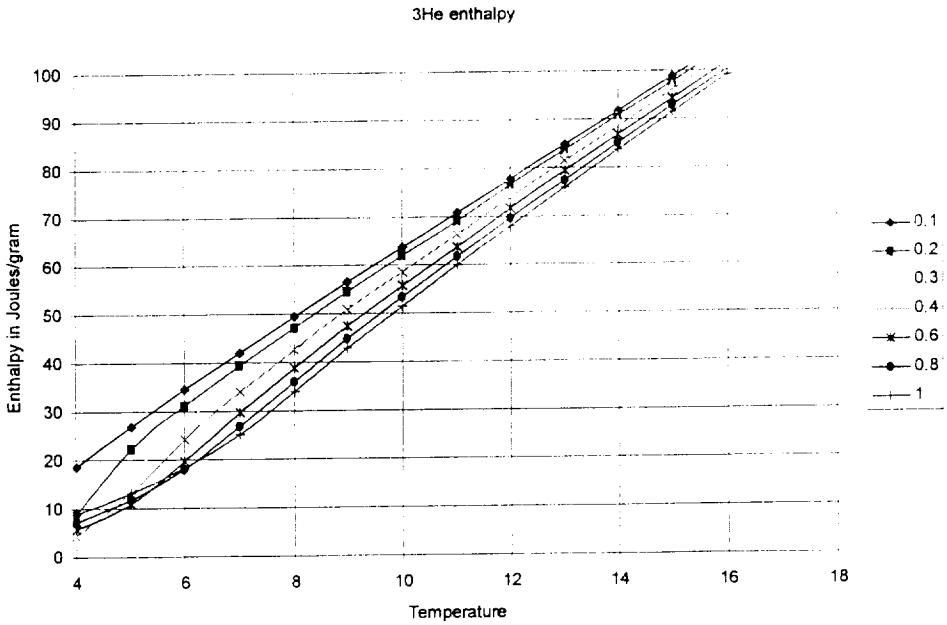

Figure 53. Enthalpy for ^{3}He gas from 4-16K, and from 1-10 atmospheres.

Note that the enthalpy per gram is greater than that of 4He. This simply reflects the fact that 1 gram of 3He has 8.3% more particles than a gram of 4He. We note a slight shift of the crossover point to below 6K, and that the reduction of enthalpy takes place at 7 bar, perhaps an atmosphere greater than the corresponding point for 4He.

Charge pressure optimization

In this section we determine the optimum charge pressure for our cooler. We are assuming that we use a variant of the 10K JT compressor, and it has a fixed pressure ratio. Therefore, the higher the charge pressure, the higher the pressure drop across the valve, and the most cooling. This continues up to the point that the JT effect saturates. We show the results of a trade study in Figure 54.

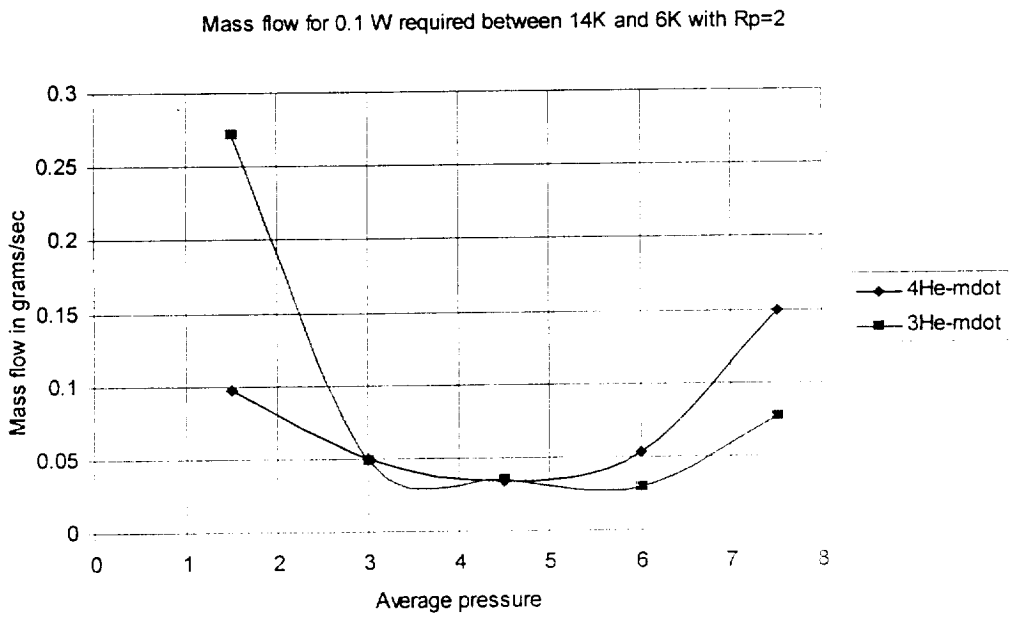

Figure 54. The optimum charge pressure is the one with the minimum flow rate while producing 100 mW of cooling.

The system prefers a mean pressure of about 4.5 Bar, corresponding to a high side pressure of 6 Bar, and a low side pressure of 3 Bar, for both 3He and 4He. The minimum reflects that the net refrigeration per gram is a maximum. At 6K the minimum mass flows for 3He and 4He are approximately the same. This puts 3He at a disadvantage because more work will have to be done at room temperature to compress the gas. We are far enough above the critical point that 3He is not yet of advantage. 4He is still active, and the enthalpy curves of 3He are not yet as splayed, resulting in a larger molar flow to equal the cooling. We therefore find that we can meet the 100 mW requirement without resorting to 3He.

Table 55. Thermodynamic design point for the 100 mW 6K cryocooler

High side valve pressure	6 Bar
Low side valve pressure	3 Bar
Mass flow	0.034 grams /second
Precooler temperature	14 K
Expansion temperature	6 K

C. Component Sizing and Parasitic Loads

We now turn to a discussion of the components required to support this ideal thermodynamic analysis. We describe the rotary vane compressor and estimate its input power. We offer "straw" designs of heat exchangers, supports, and radiation baffles, and use them to calculate parasitic loads. These will be used to establish the heat lift requirements for the Stirling precooler.

Rotary Compressor requirements

In this section we size a compressor that provides the pressures and flows assumed in our thermodynamic model. As for the heat exchangers, we scale the dimensions of an assumed geometry to meet the particular application. A full cut-away picture of our compressor is shown in Figure 4. An end view of one of the two stages is shown in Figure 56, illustrating the key parameters.

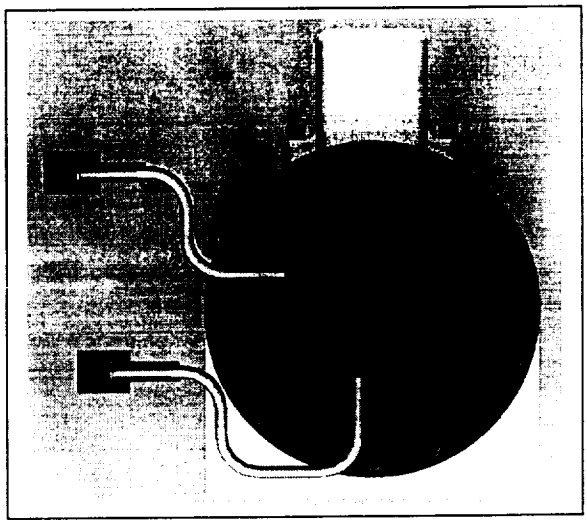

Key parameters of a rotary vane pump

- Stator radius Rs
- aspect ratio L(depth)/Rs
- vane offset os = 0
- number of vanes Nv = 6
- Location of ports $\theta i, \theta ex$
- eccentricity e = .08

Figure 56. An end view of one of two stages of the 10K rotary vane pump. The retractable vanes sweep gas from the inlet (10 o'clock) to the outlet (7 o'clock).

We developed a pump on the parallel 10K program capable of a pressure ratio of 2 and a displacement of 133 cc/second. The pump is specifically designed for dry helium, and to have a 10 year lifetime.

The 6 K compressor requires less displacement and has lighter mechanical loads due to a lower mean operating pressure. The required first stage displacement is simply the volume the pump sweeps in a second that results in a mass flow of .033 gm/sec. At 3 Bar and 273K, this equals 62 cc/second. Assuming 24 hz operation, the displacement per cycle is approximately 2.6 cc. For a pump with any number of vanes, the displacement in one revolution is approximately (2*pi*Rs)* (2*e*Rs)*L. Thermodynamically, all we need is 2.6 cc of displacement. However, we stipulate that the pump displace 4 cc to allow for internal leakage, ie., the pump would be 2/3 efficient in pumping gas. The resulting pump "speed" at 24 hz is 96 cc/sec.

Since the pump has two stages, and a pressure ratio of 2, each stage has a pressure ratio rp =Ph/Pl of 1.41. The pressure ratio is a peculiar concept in a rotary vane pump and requires some explanation. The pump intrinsically has a volume compression ratio given by the change in volume between a pair of vanes when the pair goes from the inlet to the exhaust. This number depends upon the eccentricity, the number of vanes, and the inlet and exhaust angles, which for our 10K pump are approximately 180 degrees, and 275 degrees w/r/t Top Dead Center, as shown in figure 56. The volume ratio r_v is 1.35 for the 10K pump. The pressure compression ratio depends upon extra factors, such as how adiabatic the compression is, and how much gas leaks out during compression. Determining the pressure ratio require a detailed time simulation of the compression process. Our pump could sustain a pressure ratio of 2 in a properly designed system.

We can now turn to a calculation of the compressor power. A peculiar aspect of the rotary vane pump is that the compression chamber disappears at top dead center. It therefore dumps its contents independent of the exhaust pressure. As a result, the pump runs between any inlet and exhaust pressures. This interesting situation leads to extra dissipation when the exhaust pressure doesn't match the pressure the pump naturally generates. Including this effect, a theoretical measure of the power expended is

$$\text{Power} = \text{mdot}*R*Ti *(3/2\ r_v^{\wedge 2/3} + (Pf/(r_v Pi)) - 5/2)$$

For each stage, at 20C,
Power = ({4/2.6}*.033) *(8.3/4)*293 {1.5 *(1.35)^2/3 + (1.41/1.35) -2.5} = 11.6 watts

The total pV power for two stages is twice this, or 23 watts. If we add 33% margin for extra shaft work (mechanical loss on internal parts), we estimate 30 watts on the shaft. With an 80% motor, we have to assume 38 watts into the compressor.

Table 57. Assumed compressor elements

Compressor Mass (10 K compressor)	5 Kg
Thermodynamic mass flow requirement	.033 grams/sec
Mass flow margin for leakage	(4/2.6)* .033 g/sec = .051 grams/sec
PV power for two stages	23 watts
Shaft power other than pv (Margin)	+ 7 watts = 30 watts
Motor efficiency	80%
Compressor electrical power	38 watts
+Electronics = 10 watts tare + 86 % eff	54 watts electrical including controller

Cold Head design

We now turn to the detailed design of the cold head, which consists of the heat exchangers, baffling, and support structure required by the 6K cooler. In this section we assume an efficiency for our heat exchangers, and show that it can be met with a geometry under development at the National Institute for Science and Technology.

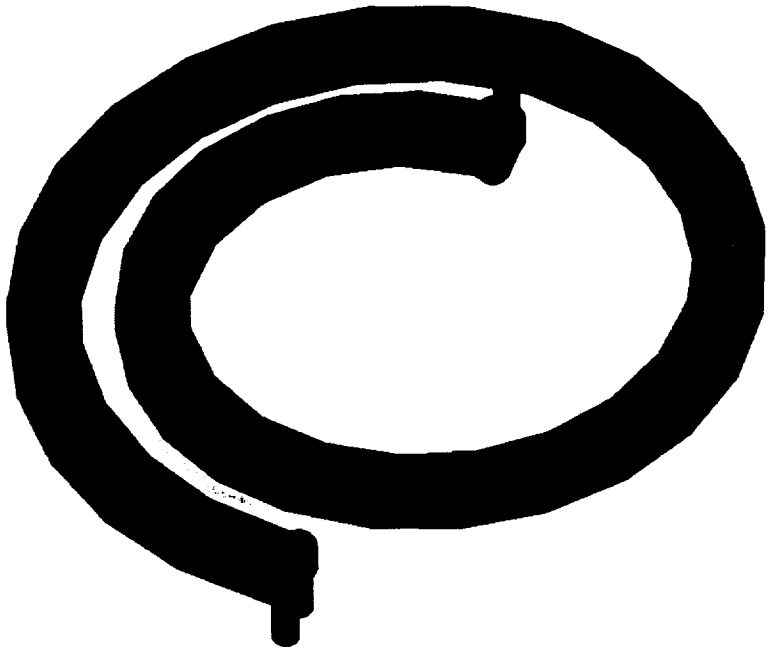

Figure 58. Exchangers proposed for the 6K cryocooler consist of multiple stainless steel layers configured in a flat spiral geometry.

We assume that the exchangers achieve 99% efficiency, ie the total parasitic heat loads on the cold end are 1% of the enthalpy transport mdotCp*ΔT, the amount of heat that has to pass laterally from the inlet stream to the outlet stream. We arbitrarily increase the mass flow from 33 mg/sec to 40 mg/sec for efficiency margin.

Table 59. Assumed heat exchanger thermodynamic requirements

Exchanger	ε %	Mass flow	Transfer	Heat leak	ΔP	Ave pressure
300-180K	99	.040 g/s	25 watts	.25 watts	3 psi/ 2 psi	6 Bar/ 3 Bar
180K-40K	"	"	29 watts	.29 watts	2psi/ 1.5 psi	6 Bar/ 3 Bar
40K- 14 K	"	"	5.4 watts	.176 watts	1.5psi/ 1 psi	6 Bar/ 3 Bar

A section of the spiral ribbon is shown below. It consists of diffusion bonded stainless steel sheets that have had channels etched in them.

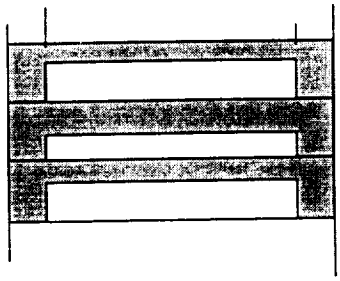

Figure 60. Section of the heat exchanger showing layered flow channels

A high pressure stream flows between low pressure streams, and transfers its heat to the flows on either side. We tailor the gap spacing, foil thickness, length, and area to arrive at a configuration whose heat load, fluid plus conduction, sums to 1% of the heat being exchanged between high and low pressure flows.

Results:

Table 61. Physical properties of the compact, multi-layered heat exchangers sized to be 99% efficient for this 100 mW application.

Exchanger	Length (cm)	Width (mm)	Mass (gm)	Hot gap spacing (in)	Cold gap Spacing(in)	# layers
300-180K	35.4	6.1	87	0.007	0.007	10
180K-40K	29.9	5.6	65	0.005	0.005	10
40K- 14 K	12.1	8.1	20	0.002	0.002	6
14-6K	7.5	6.7	11	0.001	0.001	6

If we assume that the length can be spiraled in a plane, as shown in Figure 58, we find a effective diameter of approximately 8 cm for first element. The combined mass of the system is < ¼ Kilogram.

Figure 62. A series of shields are conjured up that envelop the hybrid cooler and provide extra volume for a load. The shield areas are used to estimate parasitic radiation loads.

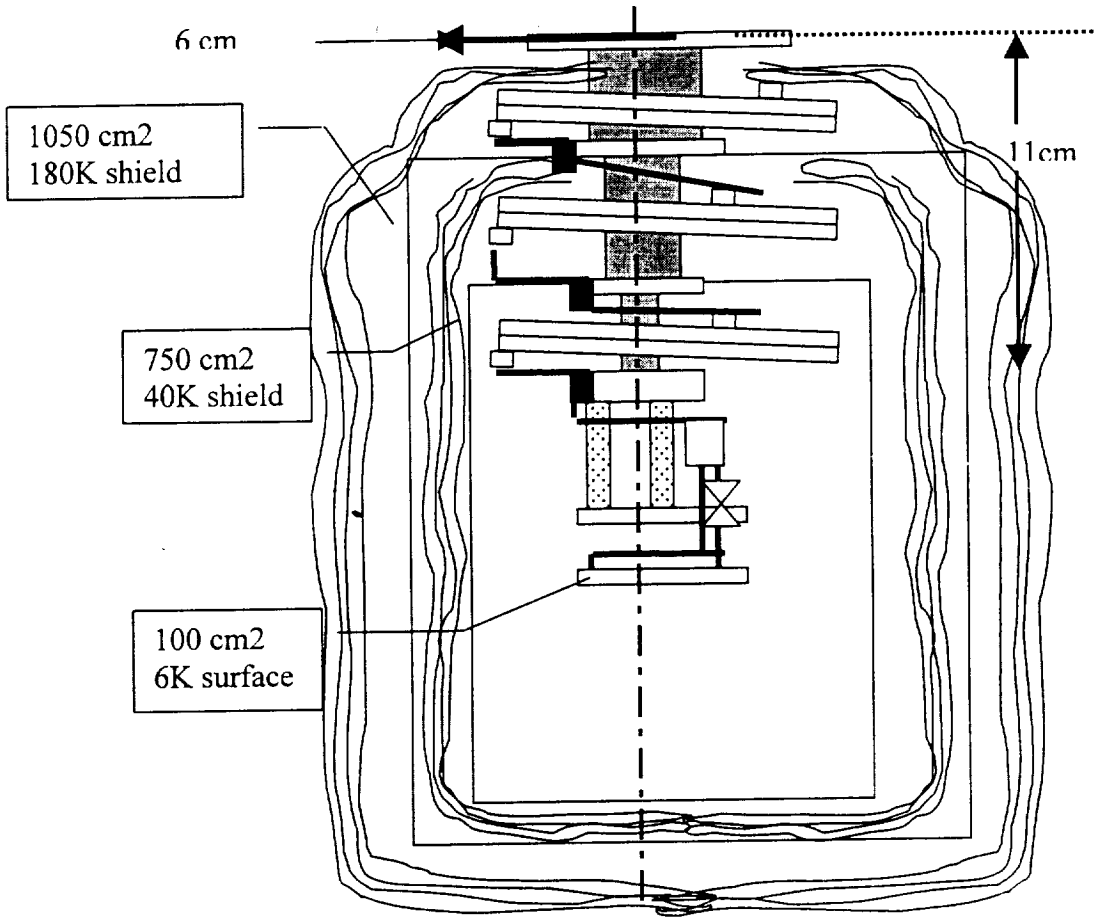

Calculated radiation loads on the various stages

Geometry for the calculation of radiation loads	Load (mW)
180K -Radiation shield at 180K surrounded by 20 layer MLI blanket -300-180 K spiral heat exchanger wrapped with 5 layer MLI blanket	600 mW
40K -Radiation shield at 40K, surrounded by a 20 layer MLI blanket -180-40 K Spiral heat exchanger wrapped with 5 layer MLI blanket	60 mW
6 K 100 cm2 combined area of JT valve and heat exchanger , no MLI	.3 mW

Notes:
Source emissivity assumed to be 0.2 = 6.6 x polished aluminum
Radiation load is reduced by 1/Nlayers

Mechanical supports and their thermal consequences

This section is necessarily vague, because the support structure will depend upon the load and how it is supported. Although the coldfinger can support the cold head quite comfortably in a lab environment, it can't handle the loads generated during launch vibrations. A reasonable estimate of the radiation shields shown in the figure is close to 400 grams, and inertial loads could be 60 Newtons or more.

However, we can make a crude estimate of the thermal loads required by a generic support structure. We recognize that the main new elements are mechanical supports required to take the forces generated by the launch vibrations. We have designed such a structure on the HIRDLS program, where we supported a long thermal rod and several s links with our Stirling cold finger.

In that application we used Kevlar brace cables in tension to support the mass. We used a group of 6 straps to support loads and moments. Each strap was capable of > 400 lbs. We postulate a similar set and estimate their heat leak. This essentially is a place holder for a similar structure designed around a real load.

Kevlar's conductivity is .01 W/cm K at 60K, .015 W/cm K at 180K, and .02 W/cm K at 300K. Assuming a bundle 5 cm long (perhaps by arranging for a re-entrant connection), and .05 cm2 in area (a bundle of 5000 12 micron diameter filaments), we find for a 100 K temperature gradient a heat leak of Q= .01*(.05/5)*100 = 10 mW per "strap". We calculate the conduction through 6 straps, assuming straps run between our stages, and making allowances for the change of conductivity with temperature.

SUMMARY OF THE HYBRID COOLER DESIGN SECTION

Table 63 Final estimate of loads to be carried by the Stirling cooler.

	180K stage	40 K stage	14 K stage	6 K stage
Radiation	600 mW	60 mW	.3 Mw	.3 mW
Structural	130 mW	72 mW	16 mW	5 mW
JT heat exchanger	250 mW	290 mW	176 mW	
Load with Margin (33%)	1.3 watts	0.56 watts	0.192 watts	7 mW

D. Stirling Precooler Design

In this section we turn the heat loads acquired in our system model into a Stirling Precooler. We then estimate the input power and size of this precooler.

Prediction process

Our math models predict the thermo-physical behavior of a cooler once its geometry is specified. Because of this, our design algorithm is the "time honored guess and check" method outlined below. We begin with a list of key cooler parameter values, essentially the numbers on the data sheet in the test plan for each test we ran. The thermo-mechanical model gives us pV diagrams and mass flows. Cold head construction details give us the conduction and shuttle losses. And Regen3.1, the program we validated with our regenerator tests, provides the regenerator losses. The parameter set is adjusted until the net cooling is consistent with our thermal requirements.

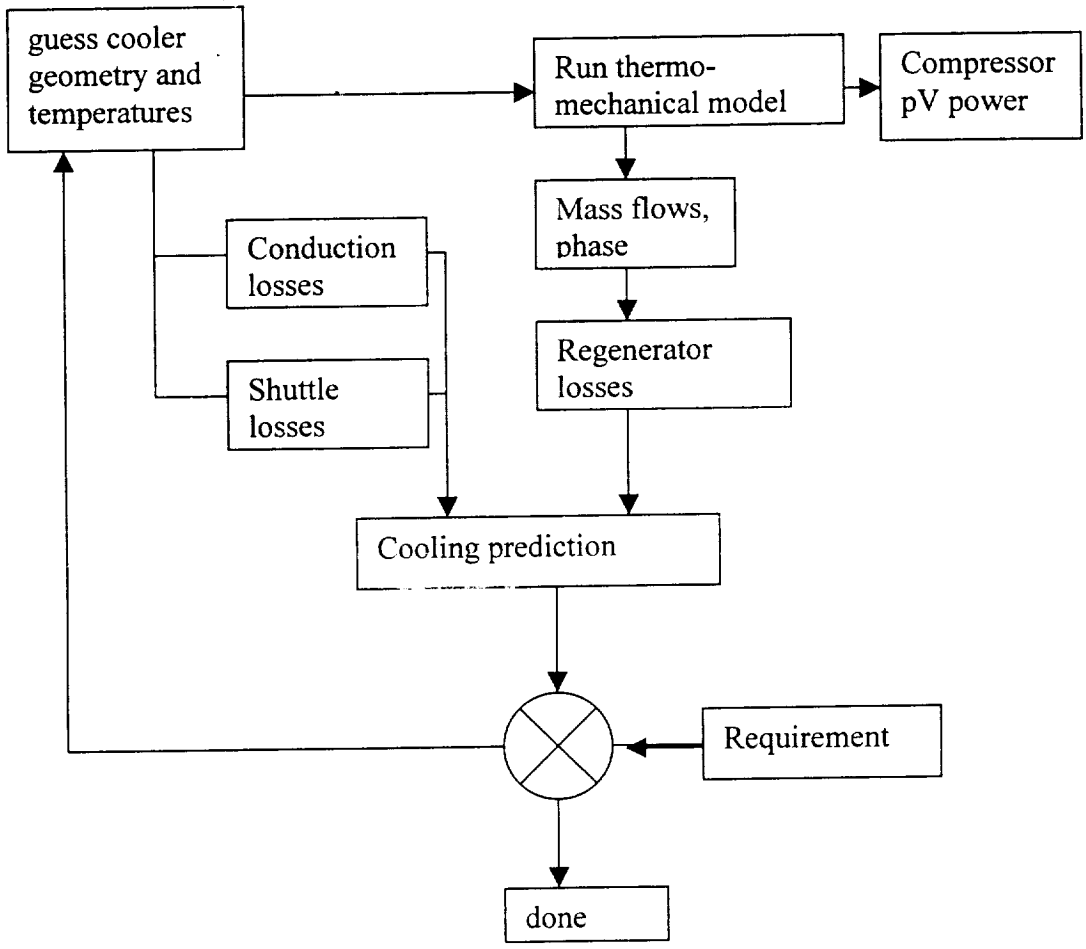

Figure 64. The Stirling cooler design algorithm.

The process is complex because we have three simultaneous loads to satisfy. We find that it is convenient to assume low and high temperatures for the upper most stage, and extrapolate to the temperature Tm that meets the load requirement. This means that we don't quite meet the stated temperature of 180K at our heat sink, but that does not usually affect the loads in a significant way. We illustrate the process in the figure below.

Also, the design is not complete simply because we meet the requirements. Once our design provides the required cooling, it is necessary to vary the parameters in such a way that we maintain the cooling but lower the input power. This optimization phase results in a better cooler. The cooler outlined here has been optimized to some degree, but still should be considered a preliminary design.

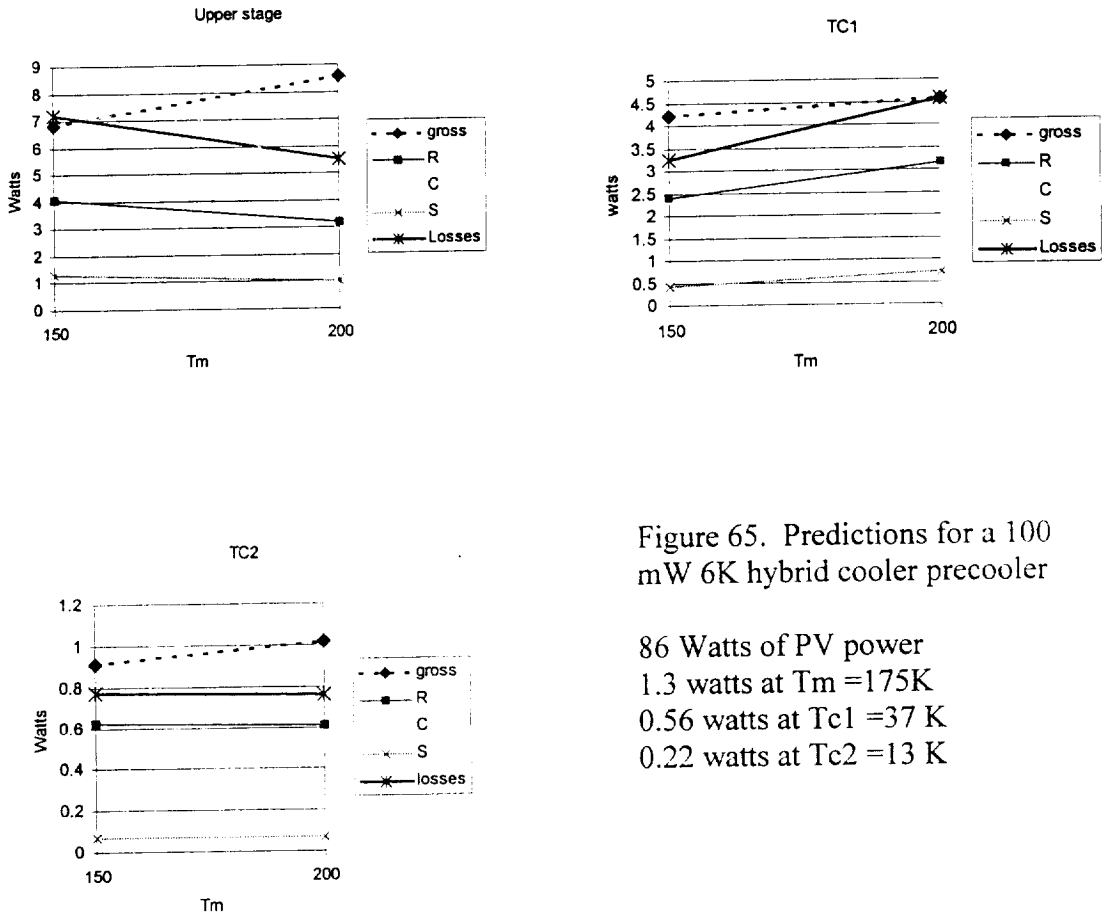

Figure 65. Predictions for a 100 mW 6K hybrid cooler precooler

86 Watts of PV power
1.3 watts at Tm =175K
0.56 watts at Tc1 =37 K
0.22 watts at Tc2 =13 K

Table 66. Precooler parameters in the format of the parameter set in the test reports.

SB235 type Compressor parameters:

Diameter	3.0	Cm
100% Stroke	1.2	cm pp each of 2
Coil resistance	0.5	Ohms
Motor constant	11.3	Nt./amp

Transfer line:

Length external to body	20 cm
Transfer line ID	.44 cm

Displacer piston: 100% PP stroke = 0.381 cm

	Diameter	Length	Radial clearance
Shaft piston	1 cm	2 cm	
First stage	2.95 cm	4.5 cm	
Second stage	2.18 cm	5.5 cm	
Third stage	1.00 cm	2.4 cm	

Regenerator

	Type	Outer diameter	Inner diameter	Length	Porosity	Frontal area	Hydraulic radius
1st stage warm	250T	3.62 cm	2.99 cm	2.25cm	.75	3.47 cm2	
1st stage cold	"	"	"	"	"	"	
2nd stage warm	250 P	2.8 cm	2.22 cm	2.75 cm	.65	2.44 cm2	
2nd stage cold	"	"	"	"	"	"	
3rd stage warm	Reay	1.88 cm	1.04 cm	1.2 cm	.38	2 cm2	
3rd stage cold	Reay	"	"	"	.38	2 cm2	

This cooler is significantly larger than our breadboard 35/60K cryocooler, but is quite comparable to our latest SB235 cooler developed on Ball IR&D. That cooler is designed to lift 1 watt at 35K, and 2.2 Watts at 100K, for an input power of about 100 watts to the compressor. I have assumed a SB235 motor, which will be 80% efficient under these conditions. The displacer will differ in that the 6K cold head is a three stage device, but the SB235 is a two stage device. However, they are still of a comparable size, and nuances in the thermal design have virtually no influence on the mass and power required by the displacer drive mechanism. We shall adopt actual mass values for the SB235 cooler displacer.

Table 67. Project total system power for the Stirling

Compressor pV (shaft) power	86 watts
Compressor input power	108 watts
+ Motor driver	119 watts
+E200 electronic tare (incl. Displacer drive)	132 watts
+Dc/dc isolation	147 watts

E. System Performance Predictions

Table 68. System performance prediction for a 100 mW 6 K cryocooler.

	Power	Mass
Stirling	147 watts	16 Kg
JT compressor	52 watts	5 Kg
Cold head	-	0.7 Kg + 1.3 Kg contamination filters
Total	200 watts	23 Kg

The mass and power in this estimate include allotments for the support and shielding of a load at 6K.